REVIEWS IN MINERALOGY AND GEOCHEMISTRY

VOLUME 58 2005

LOW-TEMPERATURE THERMOCHRONOLOGY: TECHNIQUES, INTERPRETATIONS, AND APPLICATIONS

EDITORS:

Peter W. Reiners *Yale University, New Haven, Conneticut*

Todd A. Ehlers *University of Michigan, Ann Arbor, Michigan*

COVER: ***Upper left***: Apatite crystals from the Bighorn Mountains, Wyoming (scale bar is 300 μm). ***Upper right***: Arrhenius plot for step-heating helium diffusion experiment on titanite crystal fragments; after Reiners PW, Farley KA (1999) He diffusion and (U-Th)/He thermochronometry of titanite. *Geochim Cosmochim Acta* 63:3845-3859. ***Lower left***: 3D thermo-kinematic model of the Himalayan front and major structures, Central Nepal; courtesy of D. Whipp and T. Ehlers. ***Lower right***: View of the Washington Cascades, from Sahale Arm; photo by Drew Stolar.

Series Editor: ***Jodi J. Rosso***

MINERALOGICAL SOCIETY OF AMERICA
GEOCHEMICAL SOCIETY

REVIEWS IN MINERALOGY AND GEOCHEMISTRY

(Formerly: REVIEWS IN MINERALOGY)

ISSN 1529-6466

Volume 58

Low-Temperature Thermochronology: Techniques, Interpretations, and Applications

ISBN 093995070-7

Additional copies of this volume as well as others in this series may be obtained at moderate cost from:

THE MINERALOGICAL SOCIETY OF AMERICA
3635 CONCORDE PARKWAY, SUITE 500
CHANTILLY, VIRGINIA, 20151-1125, U.S.A.
WWW.MINSOCAM.ORG

DEDICATION

Dr. William C. Luth has had a long and distinguished career in research, education and in the government. He was a leader in experimental petrology and in training graduate students at Stanford University. His efforts at Sandia National Laboratory and at the Department of Energy's headquarters resulted in the initiation and long-term support of many of the cutting edge research projects whose results form the foundations of these short courses. Bill's broad interest in understanding fundamental geochemical processes and their applications to national problems is a continuous thread through both his university and government career. He retired in 1996, but his efforts to foster excellent basic research, and to promote the development of advanced analytical capabilities gave a unique focus to the basic research portfolio in Geosciences at the Department of Energy. He has been, and continues to be, a friend and mentor to many of us. It is appropriate to celebrate his career in education and government service with this series of courses in cutting-edge geochemistry that have particular focus on Department of Energy-related science, at a time when he can still enjoy the recognition of his contributions.

LOW-TEMPERATURE THERMOCHRONOLOGY:
TECHNIQUES,INTERPRETATIONS,ANDAPPLICATIONS

58 *Reviews in Mineralogy and Geochemistry* **58**

FROM THE SERIES EDITOR

This volume, *Low-Temperature Thermochronology: Techniques, Interpretations, and Applications*, was prepared in advance of a short course of the same title, sponsored by MSA and presented at Snowbird, Utah, October 13-15, 2005 prior to the fall GSA meeting in Salt Lake City, Utah. The editors, Peter Reiners (Yale University) and Todd Ehlers (University of Michigan), carefully selected a diverse group of authors in order to produce this volume that assesses the current state-of-the-art in low-temperature thermochronology and provides a convienent context for evaluating advances in analytical and interpretation techniques, future potential, and outstanding issues in the field that have emerged in recent years. The editors and contributing authors have done an excellent job in generating this volume that should find broad use by researchers seeking to incorporate low-temperature thermochronologic constraints in their research.

Readers are encouraged to visit the MSA website (*http://www.minsocam.org/MSA/RIM/*) in order to access the computer programs outlined in Chapter 22. Errata (if any) can be found at the MSA website *www.minsocam.org*.

Jodi J. Rosso, Series Editor
West Richland, Washington
August 2005

PREFACE

The publication of this volume occurs at the one-hundredth anniversary of 1905, which has been called the *annus mirabilus* because it was the year of a number of enormous scientific advances. Among them are four papers by Albert Einstein explaining (among other things) Brownian motion, the photoelectric effect, the special theory of relativity, and the equation $E = mc^2$. Also of significance in 1905 was the first application of another major advance in physics, which dramatically changed the fields of Earth and planetary science. In March of 1905 (and published the following year), Ernest Rutherford presented the following in the Silliman Lectures at Yale:

> *"The helium observed in the radioactive minerals is almost certainly due to its production from the radium and other radioactive substances contained therein. If the rate of production of helium from known weights of the different radioelements were experimentally known, it should thus be possible to determine the interval required for the production of the amount of helium observed in radioactive minerals, or, in other words, to determine the age of the mineral."*
>
> *Rutherford E (1906) Radioactive Transformations. Charles Scriber's Sons, NY*

Thus radioisotopic geochronology was born, almost immediately shattering centuries of speculative conjectures and estimates and laying the foundation for establishment of the

1529-6466/05/0058-0000$05.00 DOI: 10.2138/rmg.2005.58.0

geologic timescale, the age of the Earth and meteorites, and a quantitative understanding of the rates of processes ranging from nebular condensation to Quaternary glaciations.

There is an important subplot to the historical development of radioisotopic dating over the last hundred years, which, ironically, arises directly from the subsequent history of the U-He dating method Rutherford described in 1905. Almost as soon as radioisotopic dating was invented, it was recognized that the U-He [or later the (U-Th)/He method], provided ages that were often far younger than those allowed by stratigraphic correlations or other techniques such as U/Pb dating. Clearly, as R.J. Strutt noted in 1910, He ages only provided "minimum values, because helium leaks out from the mineral, to what extent it is impossible to say" (Strutt, 1910, Proc Roy Soc Lond, Ser A 84:379-388). For several decades most attention was diverted to U/Pb and other techniques better suited to measurement of crystallization ages and establishment of the geologic timescale.

Gradually it became clear that other radioisotopic systems such as K/Ar and later fission-track also provided ages that were clearly younger than formation ages. In 1910 it may have been impossible to say the extent to which He (or most other elements) leaked out of minerals, but eventually a growing understanding of thermally-activated diffusion and annealing began to shed light on the significance of such ages. The recognition that some systems can provide cooling, rather than formation, ages, was gradual and diachronous across radioisotopic systems. Most of the heavy lifting in this regard was accomplished by researchers working on the interpretation of K/Ar and fission-track ages.

Ironically, Rutherford's He-based radioisotopic system was one of the last to be quantitatively interpreted as a thermochronometer, and has been added to K/Ar (including $^{40}Ar/^{39}Ar$) and fission-track methods as important for constraining the medium- to low-temperature thermal histories of rocks and minerals.

Thermochronology has had a slow and sometimes fitful maturation from what were once troubling age discrepancies and poorly-understood open-system behaviors, into a powerful branch of geochronology applied by Earth scientists from diverse fields. Cooling ages, coupled with quantitative understanding of crystal-scale kinetic phenomena and crustal- or landscape-scale interpretational models now provide an enormous range of insights into tectonics, geomorphology, and subjects of other fields. At the same time, blossoming of lower temperature thermochronometric approaches has inspired new perspectives into the detailed behavior of higher temperature systems that previously may have been primarily used for establishing formation ages. Increased recognition of the importance of thermal histories, combined with improved analytical precision, has motivated progress in understanding the thermochronologic behavior of U/Pb, Sm/Nd, Lu/Hf, and other systems in a wide range of minerals, filling out the temperature range accessible by thermochronologic approaches. Thus the maturation of low- and medium-temperature thermochronology has led to a fuller understanding of the significance of radioisotopic ages in general, and to one degree or another has permeated most of geochronology.

Except in rare cases, the goal of thermochronology is not thermal histories themselves, but rather the geologic processes responsible for them. Thermochronometers are now routinely used for quantifying exhumation histories (tectonic or erosional), magmatism, or landscape evolution. As thermochronology has matured, so have model and interpretational approaches used to convert thermal histories into these more useful geologic histories. Low-temperature thermochronology has been especially important in this regard, as knowledge of thermal processes in the uppermost few kilometers of the crust require consideration of coupled interactions of tectonic, geodynamic, and surface processes. Exciting new developments in these fields in turn drive improved thermochronologic methods and innovative sampling approaches.

The chapters

This volume presents 22 chapters covering many of the important modern aspects of thermochronology. The coverage of the chapters ranges widely, including historical perspective, analytical techniques, kinetics and calibrations, modeling approaches, and interpretational methods. In general, the chapters focus on intermediate- to low-temperature thermochronometry, though some chapters cover higher temperature methods such as monazite U/Pb closure profiles, and the same theory and approaches used in low-temperature thermochronometry are generally applicable to higher temperature systems. The widely used low- to medium-temperature thermochronometric systems are reviewed in detail in these chapters, but while there are numerous chapters reviewing various aspects of the apatite (U-Th)/He system, there is no chapter singularly devoted to it, partly because of several previous reviews recently published on this topic.

Chapter 1 by Reiners, Ehlers, and Zeitler provides a perspective on the history of thermochronology, comments on modern work in this field and general lessons on the potential for noise to be turned into signal. This chapter also provides a summary of the current challenges, unresolved issues, and most exciting prospects in the field.

Much of the modern understanding of kinetic controls on apparent ages, thermal histories, and sampling approaches comes from decades of progress in fission-track dating, a method that remains as essential as ever, partly because of the power of track-length measurements and the depth of (at least empirical) understanding of the kinetics of track annealing. Tagami, Donelick and O'Sullivan review the fundamentals of modern fission-track dating (Chapter 2). Two of the most commonly dated, well-understood, and powerful minerals dated by fission-track methods are apatite and zircon, and the specifics of modern methods for these systems and their kinetics are reviewed by Donelick, O'Sullivan, and Ketcham (Chapter 3), and Tagami (Chapter 4).

Although $^{40}Ar/^{39}Ar$ and (U-Th)/He dating methods followed somewhat different paths to their modern thermochronologic incarnations, they have many features in common, especially in the kinetics of diffusion and closure. Zeitler and Harrison review the concepts underlying both $^{40}Ar/^{39}Ar$ and (U-Th)/He methods (Chapter 5). Zircon was one of the first minerals dated by the (U-Th)/He method, but has only just begun to be used for thermochronometry of both bedrock and detrital samples, as reviewed by Reiners (Chapter 6). Continuous time-temperature paths from intracrystalline variations of radiogenic Ar proven perhaps the most powerful of all thermochronologic approaches, and an innovative analogous approach in He dating ($^{4}He/^{3}He$ thermochronometry) is revealing remarkably powerful constraints on the extreme low temperature end of thermal histories, as reviewed by Shuster and Farley (Chapter 7).

Thermochronology of detrital minerals provides unique constraints on the long-term evolution of orogens, sediment provenance, and depositional age constraints, to name a few. Bernet and Garver (Chapter 8) review the essentials of detrital zircon fission-track dating, one of the most venerable and robust of detrital thermochronometers, and in Chapter 9, Hodges, Ruhl, Wobus, and Pringle review the use of $^{40}Ar/^{39}Ar$ dating of detrital minerals, demonstrating the power of detrital muscovite ages in illuminating variations in exhumation rates in catchments over broad landscapes.

(U-Th)/He thermochronometry presents several unique interpretational challenges besides new kinetics and low temperature sensitivity. One of these is long-alpha stopping distances, and its coupling with diffusion and U-Th zonation in age corrections. Dunai reviews modeling approaches to deal with these issues in interpreting low-temperature thermal histories (Chapter 10). Ketcham (Chapter 11) reviews the theory and calibration of both forward and inverse models of thermal histories from fission-track and (U-Th)/He data, and makes some important points about the interpretations of such models.

Translating thermal histories into exhumational histories and their tectonic or geomorphic significance across a landscape requires quantitative understanding of the thermal structure of the crust and how it is perturbed, a review of which is presented by Ehlers (Chapter 12). Braun (Chapter 13) illustrates the power of low-temperature thermochronometry to constrain topographic evolution of landscapes over time, using PECUBE. Gallagher, Stephenson, Brown, Holmes, and Ballester present a novel method of inverse modeling of fission-track and (U-Th)/He data for thermal histories over landscapes (Chapter 14).

Continuous time-temperature paths from closure profiles or their step-heating-derived equivalents are, to some degree, the holy grail of thermochronology. Harrison, Zeitler, Grove, and Lovera (Chapter 15) provide a review of the theory, measurement, and interpretation of continuous thermal histories at both intermediate and high temperatures, derived from both K-feldspar $^{40}Ar/^{39}Ar$ and monazite U/Pb dating.

Extensional orogens provide a special challenge and opportunity for thermochronometry because tectonic exhumation by footwall unroofing often outstrips erosional exhumation, and often occurs at high rates. As Stockli shows (Chapter 16) thermochronology in these setting provides opportunities to measure rates of a number of important processes, as well as obtain a snapshot of crustal thermal structure and its imprint on thermochronometers with varying closure temperatures. Spotila (Chapter 17) reviews the use of thermochronology applied to tectonic geomorphology in a wide range of orogenic settings, introducing the concept of denudational maturity.

Thermochronology has found great utility in economic geology, and newly developed approaches pose great potential in this area, and shown by McInnes, Evans, Fu, and Garwin in their review of the use and modeling of thermochronology of hydrothermal ore deposits (Chapter 18). The thermal histories of sedimentary basins are also critical to understanding thermal maturation of hydrocarbons, but are also critical for understanding basin formation, erosional histories of source regions, fluid flow, and climate change and other temporal signals preserved in sedimentary rocks. Armstrong (Chapter 19) reviews these issues and the use of thermochronology in deducing the thermal histories of sedimentary basins. Drawing on large datasets of bedrock apatite fission-track dates, Kohn, Gleadow, Brown, Gallagher, Lorencak, and Noble demonstrate the power of modeling, and, importantly, effectively visualizing, integrated thermotectonic and denudational histories over large regions (Chapter 20).

Thermal histories of meteorites provide constraints on a wide range of fundamentally important processes, including nebular condensation and early solar-system metamorphic histories, and the dynamics of interplanetary collisions and shock metamorphism. Min reviews thermochronologic approaches to understanding meteorite thermal histories (Chapter 21), including new methods and approaches.

Finally, the importance of robust models with which to interpret thermochronologic data is underscored by the review of the Software for Interpretation and Analysis of Thermochronologic Data (Chapter 22), summarized and compiled by Ehlers, for programs associated with the work of authors in this volume and others. The programs outlined in this chapter are available for download through the RiMG Series website: *http://www.minsocam.org/MSA/RIM/*.

Acknowledgments

There are numerous individuals and groups deserving of thanks for this *Thermochronology* RiMG volume for their efforts from the point of initial conception through final publication the convening of the shortcourse.

We gratefully acknowledge the generous financial support of the U.S. Department of Energy, and National Science Foundation in sponsoring the short course, as well as

contributions from Apatite-to-Zircon, Inc., the Yale Department of Geology and Geophysics, and the University of Michigan Department of Geological Sciences.

We appreciate helpful chapter reviews from all the reviewers, whose efforts helped make this a real community project. They include: Bruce Idleman, Barry Kohn, Diane Seward, Kerry Gallagher, Richard Stewart, John Garver, Ethan Baxter, Danny Stockli, Raphael Pik, Andy Carter, Max Zattin, Mike Cosca, Fin Stuart, Cristina Persano, Marlies ter Voorde, Dale Issler, Ed Sobel, Kevin Furlong, Phil Armstrong, Jean Braun, Mark Brandon, Peter Van der Beek, Terry Spell, Kip Hodges, Uwe Ring, Annia Fayon, Laura Webb, Anthony Harris, Ken Hickey, Peter Kamp, Paul O'Sullivan, Geoff Batt, Paul Andriessen, Mario Trieloff, Francis Albarède, Phaedra Upton, Stuart Thomson, Andrew Meigs, Barbara Carrapa, Tibor Dunai, Ann Blythe, and the anonymous reviewers.

We appreciate the patient and wise counsel of Alex Speer who helped us navigate the logistics of the volume and shortcourse; John Valley also provided helpful encouragement and advice in the early stages. We also thank Jodi Rosso for thoroughly professional and efficient editorial handling of the production phase of the volume. We appreciate the perspective and advice of Peter Zeitler has provided to us in putting together this volume and shortcourse, and are grateful to him and all the other veterans of the field who have encouraged and inspired us and many other researchers to enter into the great thermochronologic conversation. We hope that this volume will likewise encourage continued innovation and discoveries in this field that synergizes the work and imaginations of geochemists, geodynamicists, tectonicists, geomorphologists, and others.

August 2005

Peter W. Reiners
New Haven, CT

Todd A. Ehlers
Ann Arbor, MI

TABLE OF CONTENTS

1 Past, Present, and Future of Thermochronology

Peter W. Reiners, Todd A. Ehlers, Peter K. Zeitler

2 Fundamentals of Fission-Track Thermochronology

Takahiro Tagami, Paul B. O'Sullivan

3 Apatite Fission-Track Analysis

Raymond A. Donelick, Paul B. O'Sullivan
Richard A. Ketcham

4 Zircon Fission-Track Thermochronology and Applications to Fault Studies

Takahiro Tagami

5 Fundamentals of Noble Gas Thermochronometry

T. Mark Harrison, Peter K. Zeitler

9 $^{40}Ar/^{39}Ar$ Thermochronology of Detrital Minerals

K.V. Hodges, K.W. Ruhl, C.W. Wobus, M.S. Pringle

10 Forward Modeling and Interpretation of (U-Th)/He Ages

Tibor J. Dunai

11 Forward and Inverse Modeling of Low-Temperature Thermochronometry Data

Richard A. Ketcham

12 Crustal Thermal Processes and the Interpretation of Thermochronometer Data

Todd A. Ehlers

13 Quantitative Constraints on the Rate of Landform Evolution Derived from Low-Temperature Thermochronology

Jean Braun

14 Exploiting 3D Spatial Sampling in Inverse Modeling of Thermochronological Data

Kerry Gallagher, John Stephenson, Roderick Brown, Chris Holmes, Pedro Ballester

15 Continuous Thermal Histories from Inversion of Closure Profiles

T. Mark Harrison, Marty Grove, Oscar M. Lovera, Peter K. Zeitler

18 Application of Thermochronology to Hydrothermal Ore Deposits

Brent I. A. McInnes, Noreen J. Evans, Frank Q. Fu, Steve Garwin

19 Thermochronometers in Sedimentary Basins

Phillip A. Armstrong

20 Visualizing Thermotectonic and Denudation Histories Using Apatite Fission Track Thermochronology

Barry P. Kohn, Andrew J.W. Gleadow, Roderick W. Brown, Kerry Gallagher, Matevz Lorencak, Wayne P. Noble

21 Low-Temperature Thermochronometry of Meteorites

Kyoungwon Min

22 Computational Tools for Low-Temperature Thermochronometer Interpretation

Todd A. Ehlers, Tehmasp Chaudhri, Santosh Kumar, Chris W. Fuller, Sean D. Willett, Richard A. Ketcham, Mark T. Brandon, David X. Belton, Barry P. Kohn, Andrew J.W. Gleadow, Tibor J. Dunai, Frank Q. Fu

Reviews in Mineralogy & Geochemistry
Vol. 58, pp. 1-18, 2005

Past, Present, and Future of Thermochronology

Peter W. Reiners
Dept. of Geology and Geophysics
Yale University
New Haven, Connecticut, 06520, U.S.A.
peter.reiners@yale.edu

Todd A. Ehlers
Dept. of Geological Sciences
University of Michigan
Ann Arbor, Michigan, 48109, U.S.A.
tehlers@umich.edu

Peter K. Zeitler
Dept. of Earth and Environmental Science
Lehigh University
Bethlehem, Pennsylvania, 18015, U.S.A.
peter.zeitler@lehigh.edu

INTRODUCTION

In one form or another, geochronologists have been practicing thermochronology[1], the use of radioisotopic dating to constrain thermal histories of rocks and minerals, for over 40 years. Building from lessons learned over these four decades, thermochronology continues to evolve due to technical developments, increasingly sophisticated theoretical models, and an expanding range of applications in geologic and planetary science. Most recently, interest in earth-surface processes and interactions between tectonics, erosion, and climate has drawn attention to techniques that can address the timing and rates of processes operating at temperatures below about 300 °C.

The purpose of this RiMG volume is to assess the current state of thermochronology, as of *circa* 2005, which is, coincidentally, the 100th anniversary of the first radioisotopic date (Rutherford 1905; 1906). Excellent review papers and books on specific topics within this field have been published, but no single volume has yet provided a comprehensive review of current practices, basic theory, and illustrative examples. The motivation for this volume stems from these considerations. Knowing that in a fast-developing field a book like this can

[1] Several nomenclative conventions have evolved around variations of the term "thermochronology." We consider the following most appropriate: 1) *Thermochronometer*: a radioisotopic system consisting of radioactive parent, radiogenic daughter or crystallographic feature, and the mineral in which they are found. 2) *Thermochronometry*: the analysis, practice, or application of a thermochronometer to understand thermal histories of rocks or minerals. 3) *Thermochronology*: The thermal history of a rock, mineral, or geologic terrane. In practice, however, *thermochronology* is often also used to denote the study of *thermochronologies*, in which case it is synomymous with *thermochronometry*. The use of the term *thermochronology* in the latter sense is too common and deeply ingrained in the community (and parallel with conventional usage of geochronology), to attempt any corrective usage recommendation (e.g., the title of this book is *Thermochronology*, referring to the study of, not specific, *thermochronologies*).

1529-6466/05/0058-0001$05.00 DOI: 10.2138/rmg.2005.58.1

quickly become dated, we tried to include sufficient review of fundamentals and the literature to offer students and new users a useful introduction to thermochronology that may have some staying power.

In this chapter, we first review the salient points of thermochronology's history before assessing our current capabilities and challenges and then taking the risk of suggesting where the field is headed. We do not provide a comprehensive history of the method that does full justice to the work of the large and growing cohort of thermochronologists. In this short space, we instead opted to give our perspectives on where the intellectual and technological roots of the discipline lie, which run deeper and go back farther than is sometimes appreciated.

Geochronology vs. thermochronology

Given that all radioisotopic systems are subject to disturbance and resetting at sufficiently high temperatures, it might be surmised that all radioisotopic dating is essentially thermochronology. Distinctions between geo- and thermochronology are indeed often fuzzy, but thermochronology is largely different in several ways. Some phases form or are stable only at temperatures much lower than the closure temperature for the isotopic system of interest (see Harrison and Zeitler 2005), effectively disqualifying them as thermochronometers. Zircon can form or dissolve in felsic magmas at temperatures where Pb diffusion rates are negligibly slow, for example, and in such cases it provides no useful thermal history information. Authigenic phosphates in supergene deposits provide an analogous example at low temperatures.

The nature of thermochronologic and geochronologic questions are also often fundamentally different. The formation age of minerals is typically irrelevant in thermochronology, whereas rates of processes are often of paramount interest. The numerical values of thermochronologic ages across an orogen, for example, may have little to no geologic significance aside from their inverted value in estimating steady-state cooling (and inferred exhumation) rates and their spatial variations. Geochronologic applications, on the other hand, aim exclusively to determine a singular absolute stratigraphic or magmatic formation age, with little direct concern for durations or rates of processes. There are exceptions to these generalizations. Thermochronology can estimate the absolute timing of events, such as bolide impacts or magmatic processes that may only reset low-temperature systems, and geochronology may estimate rates of processes such as evolutionary change or landscape fluvial incision by bracketing formation ages around paleontologic or geomorphic features. Despite this overlap, the bottom line is that thermochronology is distinguished from geochronology by its ability to resolve both temporal and thermal aspects of geologic processes, and thus both timing and rates of processes.

HISTORY

1950s and 1960s – development of fundamentals

The field of radioisotopic geochronology is now a century old (e.g., Rutherford 1905, 1906), and the understanding that diffusion is a means of resetting or perturbing ages is not a new idea either (e.g., Hurley 1954 and references therein). In the scientific boom years following the second world war, many ages were measured by an expanding range of techniques. One immediate observation was that many of the ages obtained by different techniques on the same samples did not agree and many were too young to represent formation ages. In general, geochronologists and petrologists were acutely aware that the measurements they were making might be dating processes other than rock formation, with diffusion and thermal resetting being major suspects, although radiation damage was also considered a potential culprit. This can be seen in the work of Patrick Hurley and his interpretations of

previous studies of He retention in a wide variety of minerals (Hurley 1954), in the work of Paul Damon and colleagues on He retentivity in zircon (Damon and Kulp 1957), in examinations of Ar diffusion in various rock-forming minerals (Evernden et al. 1960; Fechtig and Kalbitzer 1966; Musset 1969), and in Richard Armstrong's notion of a "metamorphic veil" (Armstrong 1966). Thermal resetting was also directly or indirectly invoked in a number of early field studies including Mason (1961) and Hurley et al. (1965) on mineral ages near the Alpine Fault, Hart (1964) and Hanson and Gast (1967) in examining suites of mineral ages near contact aureoles, and Westcott (1966), Harper (1967), Jäger et al. (1967), and Dewey and Pankhurst (1970) in interpreting regional suites of mineral ages from orogens.

Although thermal effects on radioisotopic ages were generally recognized, they received little quantitative attention in the early part of the 20th century and throughout the 1950s, as technological developments allowed both the U-Pb and K-Ar method to develop through advances in chemical methods and static gas mass spectrometry. In hindsight, given geochronologists' focus at that time in determining reliable formation ages rather than thermal histories, and given what we now know to be the greater retentivity of minerals for Pb and Ar compared to He, it is clear why these methods became dominant at a time when U-He workers were struggling with ages that were often too young. In any event, this period saw the rapid development of U-Pb and K-Ar dating and the abandonment of the U-He method. Other important technical developments towards the end of this period include the development of fission-track dating of geological materials by Chuck Naeser and Gunther Wagner (e.g., Naeser 1967; Wagner 1968; Naeser and Faul 1969), development of the Ar-Ar method [see McDougall and Harrison (1999) for a full account], and the impetus given to geochemistry by the lunar program.

By the late 1960s, all of the basic techniques that we use today were in fact in existence and most were under active development, with the exception of (U-Th)/He dating, which was seeing only sporadic use. Geochronologists were aware that high temperatures and diffusion could reset ages, they were conducting laboratory and field studies to study this phenomenon, and they were beginning to use mineral ages to constrain orogenic processes. The stage was clearly set for the development of modern thermochronology.

1970s – a decade of closure

Three developments in the 1970s were to prove essential to the birth of modern thermochronology. First, E. Jager and colleagues including Gunther Wagner, having accumulated considerable numbers of mineral ages from the Alps, concluded that they were recording the thermal history of the region, and published papers in support of this conclusion (e.g., Purdy and Jäger 1976; Wagner et al. 1977). Further, they used petrological data and petrogenetic grids to assign temperature values to specific isotopic systems. This directly leads to the notion of dating suites of minerals to establish thermal histories. Over the same interval, Chuck Naeser and colleagues were applying the fission-track method to a variety of geological settings of known thermal history such as boreholes and contact aureoles and relating their results to laboratory annealing experiments (Calk and Naeser 1973; Naser and Forbes 1976), and Berger (1975) and Hanson et al. (1975) revisited the studies of Hart (1964) and Hanson and Gast (1965) for K-Ar and Ar-Ar data. Finally and most significantly, in 1973, Martin Dodson published his landmark paper introducing the concept of closure temperature (defined as the temperature of a system at the time given by its apparent age), thereby providing a clear theoretical basis for understanding many mineral ages as cooling ages owing to the interplay between the kinetics of diffusion (or annealing) and accumulation rates in cooling radioisotopic systems (Dodson 1973, 1979; see discussion in Harrison and Zeitler 2005).

1980s – modern thermochronology is born

The first literature use of the word "thermochronology" appears in a paper by Berger and York (1981). By modern thermochronology, we mean the explicit use of kinetic data to interpret suites of isotopic ages in terms of thermal histories. During this period, Andy Gleadow and the Melbourne group pursued improvements in the interpretation of fission-track data, incorporating the use of confined track length data into their kinetic models for apatite data, and developing the notion of the partial annealing zone (PAZ) (Gleadow et al. 1993), which has been adapted to the diffusive context with the notion of the partial retention zone (PRZ) (Baldwin and Lister 1998; Wolf et al. 1998). Concurrently Mark Harrison put Ar-Ar thermochronology on a firm theoretical footing in a series of papers starting with a precocious undergraduate thesis devoted to the cooling history of the Quottoon pluton and extending through a series of contributions spanning his PhD work with Ian McDougall at the Australian National University (e.g., Harrison and Clarke 1979; Harrison et al. 1979, 1985; Harrison and McDougall 1980a,b, 1981, 1982). Martin Dodson extended his ideas about closure to include the notion of closure profiles (Dodson 1986). The end of the decade saw publication of papers which set the stage for the development of the multidomain model for K-feldspar age spectra (Gillespie et al. 1982; Zeitler 1987; Lovera et al. 1989, 1991; Richter et al. 1991), and also a paper on He diffusion in, and (U-Th)/He dating of, apatite (Zeitler et al. 1987) that engendered an appreciation for the potential utility of the method in many geologic applications. Finally, the interval spanning the 1980's some of the first applications of "detrital thermochronology" were attempted (Wagner et al. 1979; Zeitler et al. 1986, Cerveny et al. 1988).

During the 1980s some backlash and confusion developed over the significance of ages from thermally sensitive systems. Dodsonian closure temperatures, which are strictly only relevant for samples that have cooled montonically from high temperature and that have known kinetic properties and diffusion length scales, were often portrayed more like magnetic blocking temperatures; in fact many people at the time (and some still do) used "blocking temperature" to refer to isotopic closure. While the original choice of terms might have been arbitrary, at this point it is important to distinguish between systems with such high activation energies that in effect have a single "off-on" blocking temperature (like remagnetization of single-domain magnetite), and isotopic systems with more modest activation energies which allow both time and temperature to play significant roles in daughter isotope retention or fission-track annealing. The term closure properly serves to remind us that the conceptualization only applies to systems that have closed due to cooling; closure temperature has little to no relevance to interpretations of samples whose ages primarily reflect thermal histories involving reheating or prolonged isothermal stagnation.

Finally, the 1980s saw an increasing number of applied papers using mineral ages to constrain and solve tectonic problems. Most applications focused on quantifying the timing of geologic events such as when faults became active within an orogen, or the timing of exhumation. Many studies also used thermochronometers to estimate rates of tectonic processes (e.g., rates of exhumation) by assuming steady-state 1D thermal gradients and a closure temperatures. The later third of this volume discusses applications of thermochronometers to different settings and summarizes work by many different groups over the last 2 decades.

1990s and 2000s

One of the most important developments in the 1990s was the theoretical maturation of the multidomain model for K-feldspar $^{40}Ar/^{39}Ar$ age spectra, largely by the group at UCLA, and its application in a large number of regional studies (Harrison et al. 1991, 1993; Fitzgerald and Harrison 1993; Lovera et al. 1993, 1997, 2002). Time-temperature models provided by K-feldspar $^{40}Ar/^{39}Ar$ methods are in some sense the holy grail of thermochronology in that they provide continuous histories, approximations to which are often the focus of laborious

efforts of multiple thermochronometers providing single ages corresponding (theoretically) to a single temperature. K-feldspar $^{40}Ar/^{39}Ar$ dating continues to attract wide use, as well as occasional theoretical criticism (e.g., Villa 1994; Parsons et al. 1999), the merits of which are debated. Provided certain sample and analytical criteria are met (Lovera et al. 2002), there is as yet no convincing empirical evidence suggesting problems with the theory or application of multidomain K-feldspar $^{40}Ar/^{39}Ar$ thermochronometry (Harrison et al. 2005).

The 1990s also saw the pioneering work of Ken Farley and coworkers in bringing (U-Th)/He geochronology of apatite and other minerals to become routine measurements capable of exciting new applications (e.g., Farley et al. 1996; Wolf et al. 1996, 1998). Over the same time period, widespread adoption of laser heating for gas extraction (e.g., Kelley et al. 1994; House et al. 2000) and automation in noble-gas laboratories greatly reduced the effort required to obtain data, providing increased throughput, greater quality control, and lower system blanks. From a phenomenological standpoint, it is not clear whether lasers have increased insight into the workings of thermochronometers, as the nature of diffusion boundaries within mineral grains remains cryptic and often smaller and more complex than can be internally sampled using a laser on a routine basis (although there are exceptions in which crystal and domain sizes scale similarly and can be used to model thermal histories; Hess et al. 1993; Hawkins and Bowring 1999; Reiners and Farley 2001). Nevertheless, this area remains a frontier in which there is a great deal of interest and ongoing work.

A potentially promising development in radiogenic He chronometry is reminiscent of the shift from K/Ar to Ar/Ar dating in the 1960s and 70s: the bombardment of samples by high-energy protons to form abundant and homogeneously distributed ^{3}He provides the opportunity to simultaneously degas ^{3}He and ^{4}He and examine, with high precision, the internal distribution of ^{4}He within crystals (Shuster et al. 2003; Shuster and Farley 2003, 2005). Modeling intradomainal ^{4}He profiles allows detailed constraints on subtle but critical features of cooling in temperature ranges near and significantly below those of the closure temperature of the system of interest. The method has also been used to date formation of weathering horizons (Shuster et al. 2005).

Another development in this period has been the building of more complex numerical models used for interpretation of thermochronometer data. For example, forward and inverse models of thermochronologic data became available and widely used (e.g., Laslett et al. 1987; Gallagher 1995; Ketcham 1999, 2005; Willett 1997). Furthermore, forward modeling of crustal thermal fields to aid in interpretation of thermochronometer data also became more common. It is worth noting that the influence of topography, erosion, and faulting has long been appreciated in the geothermics community, going back to early publications by Lees (1910), Bullard (1938) and Benfield (1949). Unfortunately, much of the geothermics literature has been under utilized by thermochronologists until work by Parrish (1985) provided a fairly complete analysis of the implications of erosion on geotherms and thermochronometer interpretation.

In the last decade modeling approaches have moved beyond 1D applications to consider the influence of 2D and 3D heat transfer on thermochronometer age interpretation. Recognition in the thermochronology community that thermal gradients in the upper 1–5 km are spatially variable within orogens due to topography, faulting, and other processes has sparked interest in using thermochronometer data to quantify the rates of tectonics and erosional processes. As a results of this interest, thermochronometer data are now increasingly used to constrain thermal-kinematic and geodynamic models of tectonic (e.g., Rahn and Grasemann 1999; Batt et al. 2001; Beaumont et al. 2001; Ehlers 2005), topographic, and erosional processes (e.g., Stuwe et al. 1994; Mancktelow and Grasemann 1997; Ehlers and Farley 2003; Braun 2005). A more thorough discussion and overview of modeling procedures for thermochronometer grain scale and crustal processes are presented in this volume.

CURRENT PRACTICE

At present, by far the most commonly used thermochronometers are $^{40}Ar/^{39}Ar$ in micas and amphiboles (e.g., McDougall and Harrison 1999; Kelley 2002), and in K-feldspar (Harrison et al. 2005), fission-tracks in apatite (e.g., Donelick et al. 2005) and zircon (e.g., Tagami et al. 2005), and (U-Th)/He in apatite (e.g., Farley 2002) and zircon (e.g., Reiners 2005). These techniques have typical closure temperatures ranging from as high as 400–600 °C to as low as 60–70 °C (Table 1). Other thermochronometers used less commonly include fission-tracks in titanite (e.g., Coyle and Wagner 1998), (U-Th)/He in titanite (Reiners and Farley 1999; Stockli and Farley 2004), and monazite (Farley and Stockli 2002), and U/Pb or Th/Pb in monazite (Harrison et al. 2005), apatite (Chamberlain and Bowring 2001), titanite (Schmitz and Bowring 2003), and other phases. Thermochronologic constraints from U/Pb and Th/Pb work on accessory phases is seeing increasing use owing to the greater number of ion probes now available for radioisotopic dating, as well as advances in understanding of Pb diffusion (e.g., Cherniak 1993; Cherniak and Watson 2001) and closure profiles within minerals (Harrison et al. 2005).

Although not a focus of this volume, it is worth noting that the Rb/Sr (e.g., Jenkin et al. 2001), Sm/Nd, and Lu/Hf systems have also seen increasing use as thermochronometers, with the latter two finding increasing use in garnet (Scherer et al. 2001; Ducea et al. 2003) and apatite (Barfod et al. 2002). In general, the Sm/Nd, Lu/Hf, and (U-Th)/Pb systems provide relatively high temperature thermochronologic constraints (>450 °C). Their utility as thermochronometers has been facilitated in part by increased temporal resolution of high-temperature portions of time-temperature paths that have come from both increased precision and numbers of phases dated in the same rocks. The recognition that distinct systems provide ages that are consistently resolvable has helped extend the reach of thermochronology to higher temperatures (e.g., Hawkins and Bowring 1999).

In practice, given the sorts of minerals that yield consistent results and their fairly low closure temperatures, almost all thermochronological studies have been directed at the more felsic rocks of the continental crust. Minerals suitable for dating are also found in meteorites (e.g., Min 2005) and, perhaps more commonly than realized, in oceanic crust (e.g., John et al. 2004), and thermochronometry poses potential for understanding a range of processes in these settings as well.

The various papers in this volume discuss the systematics and kinetics of different mineral systems in more detail, but to provide an overview, Table 1 summarizes the approximate temperature ranges and time-temperature responses of thermochronometer systems commonly used today [also see Hodges (2003) for a more complete summary].

It is beyond the scope of this chapter to explore how well various thermochronometers perform when compared. There has been little if any community effort devoted to controlled comparisons of diffusion measurements or in developing standards to facilitate this. Although laboratories tend to use similar technologies, this is not universally the case, and most thermochronologists know of the pitfalls that can afflict, for example, the accuracy of temperature measurements made using thermocouples or pyrometers. Fortunately, the results from the numerous applied studies that have now been done suggest that to at least first order, we know the relative performance of mineral systems fairly well, as expressed by the closure temperatures listed in Table 1. It is extremely important to understand that the closure temperatures listed in this table serve as a useful shorthand for representing the "retentivity" of a system, but that in the actual case of reheating, these temperatures have little to no significance, the response of the system being a function of both the duration and magnitude of the heating event.

Table 1. Summary of commonly used thermochronometers and features.

Decay System	*Mineral*	*Approximate precision* (%, 1σ)	*Closure Temperature* (°C)	*Activation Energy* (kJ/mol)	*References*
(U-Th)/Pb	zircon	1–2	>900	550	Cherniak and Watson (2001); Cherniak (2001)
	titanite	1–2	550–650	330	Cherniak (1993)
	monazite	1–2	~700	590	Cherniak et al. (2004)
	apatite	1–2	425–500	230	Chamberlain and Bowring (2001); Cherniak et al. (1991)
$^{40}Ar/^{39}Ar$	hornblende	1	400–600	270	Harrison (1981); Dahl (1996)
	biotite	1	350–400	210	Grove and Harrison (1996); Harrison et al. (1985)
	muscovite	1	300–350	180	Robbins (1972); Hames and Bowring (1994)
	K-feldspar	1	150–350	170–210	Foland (1994); Lovera et al. (1991; 1997)
Fission-track	titanite	6	(a) 240–300 (b) 380–420	440–480	(a) Coyle and Wagner (1998); (b) Watt and Durrani (1985); Naeser and Faul (1969)
	zircon (a) zero-damage (b) "natural"	6	(a) 330–350 (b) 230	(a) 300–350 (b) 210	(a) Tagami et al. (1998); Rahn et al. (2004) (b) Brandon and Vance (1992); Brandon et al. (1998)
	apatite	8	90–120	190	Laslett et al. (1987); Ketcham et al. (1999)
(U-Th)/He	titanite	3–4	160–220	190	Reiners and Farley (1999)
	zircon	3–4	160–200	170	Reiners et al. (2004)
	apatite	3–4	55–80	140	Farley (2000)

Note: Approximate precisions are estimated values for age determinations; for TIMS U/Pb measurements precisions can be considerably better than cited here. Closure temperatures calculated using Dodson (1973) [or, for fission-track, Dodson (1979) using the 50% annealing isopleth (fanning models); also see Brandon et al. (1998)] using typical ranges of grain sizes and cooling rates (1–100 °C/m.y.) (small grains/low cooling rate and large grains fast/cooling rate). Also see Hodges (2003) for a similar and more complete compilation.

At the simplest level, thermochronometric data are used to determine the time-temperature history of a sample (e.g., Ketcham et al. 2005). After a thermal history is determined, numerical or analytical thermal models or simply geologic constraints can be used to interpret the processes responsible. Thermal models can be used to simulate the exhumation, and/or burial, history of the thermochronometric record as a function of geologic processes that are free parameters in the model. In practice, the range of geologic processes simulated in this type of model can be large and encompass geomorphic, faulting, magmatic, thermo-physical (e.g., basal heat flow) and basin evolution processes. Model thermal histories can be compared to observed thermal histories to determine the combinations of model parameters that provide a good fit to the data.

Unfortunately, interpretations of thermochronometric data are seldom unique because different combinations of model parameters (e.g., basal heat flow and erosion rate) can produce an equally good fit to the data. Thus, a rigorous interpretation of a data set usually results in the identification of *the range* of solutions that satisfy the observation rather than a single solution. Unfortunately, all too often studies that attempt to quantify, for example, the kinematic history of a fault fail to report the range of solutions that satisfy a thermochronometric data set.

Most recently, attempts have been made to couple crustal scale thermal models with increasingly complex process based models to better understand rates of landscape evolution, or the dynamics of orogenesis. The coupling of thermal and landform evolution and/or geodynamics models with thermochronometry pushes the utility of thermochronometric data to its limit. Coupled models introduce many more free parameters and require a careful evaluation of these parameters as well as large, carefully sampled data sets to ascertain meaningful results. The next decade will undoubtedly reveal the limit of thermochronometric data to quantify processes such as the evolution of drainage basins and/or couplings between climate and tectonics.

PROSPECTS

Existing and emerging techniques and approaches

It is likely that the recent trend towards highly automated sample processing and smaller sample sizes will increase sample throughput from laboratories, and this will be aided by lower costs, (e.g., if inexpensive quadrupole mass spectrometers can be shown to serve adequately for Ar-Ar as well as He work), because if the capital cost of new laboratories were lessened more facilities could be established. Should it reach a sufficient threshold, higher throughput opens the possibility of constructing synoptic data sets for critical portions of orogens, or even of whole orogens themselves. In addition, as interest in detrital thermochronology grows, there will be a great need for increased throughput in order to meet demand.

Work on laser microsampling in $^{40}Ar/^{39}Ar$ dating has revealed the potential of intracrystalline ^{40}Ar profiles to reveal details of cooling histories and other powerful constraints (e.g., Kelley and Wartho 2000). The prospect of measuring in-situ ^{4}He diffusion profiles by laser ablation may also be realized (Hodges and Boyce 2003), though several additional complications will need to overcome including complications posed by combined effects of U-Th heterogeneity and long alpha-stopping distances, as well as attaining sufficient resolution relative to the features in minerals that serve as diffusion pathways. If these hurdles can be overcome, continuous time-temperature histories at the low temperatures accessible by closure profiles in the (U-Th)/He system will be a particularly valuable tool for understanding near-surface processes. Laser profiling in single crystals has also found application in characterization of parent distributions, which can be vital for accurate alpha-ejection corrections in zoned crystals (Hourigan et al. 2005).

The application of standard radioisotopic decay schemes to "new" phases has been a standard source of progress in thermochronometry for some time and may continue to be in the future, because of the unique thermal sensitivity and natural occurrence patterns of each mineral. Specific systems that have shown particular promise recently include $^{40}Ar/^{39}Ar$ and $^{4}He/^{3}He$ thermochronometry of supergene weathering deposits (Vasconcelos 1999; Shuster et al. 2005). Development of thermochronometers with temperature sensitivities lower than that of apatite (U-Th)/He may prove powerful in some circumstances such as subsurface weathering profiles and submarine samples, but such sensitivities may also make the systems susceptible to diurnal heating or other surficial temperature fluctuations, restricting their application to certain settings. On the other hand, the sensitivity of low-temperature thermochronometers, and especially the contrasting kinetic responses of different systems, to surficial (or very nearly surficial) thermal processes, may prove valuable in understanding such phenomena if strategically applied (Mitchell and Reiners 2003; Shuster et al. 2005).

Combining multiple thermochronometers in the same samples to increase the temperature range of thermal histories is fairly common, but few examples exist of combinations of thermochronometers with electron-spin-resonance, thermoluminescence, or cosmogenic nuclide analyses that constrain rates and timing of exposure. Comparisons of erosion rates from steady-state interpretations of bedrock thermochronometric ages and both in situ and basin-scale (stream sediment sample) cosmogenic nuclide abundances have been made in several cases, often with intriguingly different erosion rate estimates over the contrasting timescales of each system (e.g., Kirchner et al. 2001; Vance et al. 2003; Stock et al. 2004). But another approach that may hold potential for understanding surface processes is measuring cosmogenic and radiogenic (and in some cases nucleogenic) abundances in the same crystals. Possible examples include ^{4}He, ^{3}He, and Ne isotopes in detrital zircons or supergene weathering deposits, to determine relationships between formation, thermochronologic, and exposure ages.

Thermochronology of detrital minerals has been used since the mid-late 1980s to constrain provenance and thermal histories of source terrains (e.g., Cerveny et al. 1988; Brandon and Vance 1992; Garver and Brandon 1994). Several new approaches have emerged recently that hold promise. One is modeling of observed probability density functions of many detrital $^{40}Ar/^{39}Ar$ grains ages from alluvium from a drainage basin, using predictions of various tectonic models combined with the basin's hypsometry (Hodges et al. 2005). While this or similar approaches have been used with zircon fission-track dating for some time, its application in detrital $^{40}Ar/^{39}Ar$ methods has been one of the fruits of vast improvements in automation and sample throughput, and once again demonstrates that in as is often the case in thermochronology, quantity has a quality all its own. Another advance in detrital thermochronology is measurement of both formation (U/Pb) and cooling ages [(U-Th)/He and/or FT] in single zircons, providing improved resolution of provenance, depositional ages, and long-term orogenic histories of source terrains (e.g., Rahl et al. 2003; Reiners et al. 2005).

Kinetics, partitioning, and other fundamentals

There are still many important unresolved issues associated with the fundamental kinetics and systematics of diffusion and annealing that to some degree limit the robustness of interpretations from thermochronology. Fission-track annealing models remain vigorously debated, especially how realistically various models capture the dynamics of long-time, low-temperature annealing that is characteristic of many slowly-cooled terrains (e.g., Ketcham et al. 1999). The precise causes of annealing kinetic variations caused by composition, radiation damage, and other effects is still somewhat primitive. The potential effects of pressure on track stability have also been recently debated (Wendt et al. 2001; Kohn et al. 2002; Vidal et al. 2002). With some exceptions, fission-track annealing is generally regarded as sufficiently complex that calibrations are largely empirical and do not seek quantitative modeling of the

mechanistic atomic scale processes that lead to annealing. Better understanding of the atomic-scale processes controlling annealing may be an area of fruitful progress.

Helium diffusion in commonly dated phases also bears several poorly understood and enigmatic phenomenon such as the >280 °C "rollover" in apatite diffusion experiments (Farley 2000, 2002), and the anomalously high (compared with later stages) rates of He diffusion observed in early stages of step heating experiments in zircon (Reiners et al. 2004), titanite (Reiners and Farley 1999), and possibly other minerals (Stockli and Farley 2002). Changes in He diffusion properties at high temperature are generally considered irrelevant to retention during cooling through lower temperatures where ages actually evolve (Farley 2000), and the anomalously high He diffusivity observed at small gas fractions during experiments can be modeled as minor amounts of gas residing in low-retentivity domains which do not significantly affect the bulk crystal's thermochronometric properties (e.g., Reiners et al. 2004). Nevertheless, it is possible that these and other poorly understood non-Arrhenius phenomena may turn out to be more important than currently realized.

Other potentially important but as yet poorly understood aspects of He diffusion that may have broader implications are crystallographic anisotropy in diffusion characteristics (Farley 2000), and the fact that ^{3}He and ^{4}He appear to diffuse from apatite at essentially the same rate (Shuster et al. 2003), rather than with the inverse-root-mass dependence expected from kinetic theory. Shuster et al. (2003) suggested that a possible reason may be that movement of He is actually limited by diffusion of crystallographic defects, not the intrinsic diffusion properties of He atoms. If this is true, it raises questions about what other features of noble gas diffusion phenomena may actually be proxies for migration of crystallographic or impurity defects in minerals and how this may affect thermochronologic interpretations.

Radiation damage has long been recognized as affecting diffusion and annealing properties that control thermochronometric systems. The effects of radiation damage on annealing and diffusion are generally most evident in zircon (e.g., Hurley 1954; Nasdala et al. 2004; Rahn et al. 2004; Reiners et al. 2004; Garver et al. 2005), partly because of the high activation barrier to annealing and high U-Th concentrations. Although quantitative understanding of these effects is relatively primitive, there is potential that in certain cases, the effects of radiation damage could be used to an advantage, by essentially providing a range of thermal sensitivities similar to multi-domain behavior in a single sample (Garver et al. 2005).

Finally, there is growing recognition of the potential importance of equilibrium partitioning of noble gases into minerals, and the relationship between this and assumptions of zero-concentration boundaries and infinite reservoirs surrounding minerals of thermochronologic interest. Baxter (2003) has reformulated some of the basic theoretical constructs of noble gas chronometers to effectively explore the relationships between "excess" Ar or He, and the efficiency with which these gases can be transported away from minerals in which they were produced during cooling and closure. Examples in recent literature of ^{40}Ar/^{39}Ar ages that make little to no sense in terms of closure temperatures and classic Dodsonian theory (Kelley and Wartho 2000; Baxter et al. 2002), show that "excess" Ar can be quantitatively interpreted to provide important insights into Ar mobility, partitioning, and geologic processes. A firmer understanding of the significance and potential utility of "excess" Ar or He awaits clever experimentation, theoretical investigations, and natural examples consistent with predictions.

Quantitative interpretations of data with numerical models

In the last decade significant advances have been made in coupling thermochronometric data with numerical models to interpret topographic, erosional, and tectonic histories of orogens. The future will likely follow this trend as computing power continues to be faster, better, and cheaper and the source code for simulating different geologic processes matures.

The development and dissemination of more powerful computer models will most likely require larger data sets and carefully planned sampling strategies to optimize the signal of interest.

A variety of computer programs are currently available for quantifying different aspects of the thermochronometric record of exhumation processes. For example, forward and inverse programs for predicting apatite fission track ages and track lengths and (U-Th)/He ages a function of temperature histories are freely available (e.g., Ehlers et al. 2003; Ketcham 2005; Dunai 2005). 2D and 3D thermal-kinematic, and 2D dynamic models of orogenesis have been successfully used to interpret thermochronometer data (e.g., Batt and Braun 1997; Batt et al. 2001; Beaumont et al. 2001; Ehlers et al. 2003; Braun 2005; Braun and Robert 2005). Several different landform evolution models are also in use to study long-term landscape evolution as a function of hillslope and fluvial processes (e.g., Braun and Sambridge 1997; Ellis et al. 1999). However, with the exception of recent work by Braun (2005), few attempts have been made so far to couple all of the previous types of models into one comprehensive tool for thermochronometric analysis. Future prospects for model intensive interpretations of thermochronometric data clearly include the development and dissemination of refined coupled landform evolution and thermal models, as well as creative applications of these models to multiple thermochronometric systems. The development of more complex numerical models will also allow additional rigor in data analysis because non-uniqueness in interpretations and more complete propagation of uncertainties can be more easily explored.

Inevitably, the increased complexity of numerical and geodynamic models for predicting and interpreting thermochronometric datasets make their routine application somewhat difficult. Historically, thermal and geodynamic modeling have often been fields of study to themselves because of the extensive time and training required to learn and practice modeling that is both geologically useful and sufficiently sophisticated to advance the field. Similarly, collection of thermochronometric data requires unique skills and time investments as well. Much of the future in creative applications of thermochronology will likely rely on either the training of students with interdisciplinary skills (e.g., data collection and programming and modeling) and/or expansion of symbiotic collaborations between modelers and analysts.

General comments on the future of thermochronology

There are challenges facing thermochronology, some of which will undoubtedly lead in surprising directions. But we suggest that many if not most of these apparent unresolved issues or outstanding problems will eventually bear fruits that expand and strengthen the field. In some ways, thermochronology is the inevitable outgrowth of the empirical and theoretical maturation of geochronology in general, as it also dealt with challenging issues. As datasets from various radioisotopic systems grew in quality and quantity, complications that once confounded explanation (such as intra- and inter-method age discrepancies or inconsistent experimental diffusion results) have, through hard-won quantitative understanding of kinetic properties, been transformed into powerful tools for piecing together detailed thermal histories. It is in this lemons-to-lemonade context that we mention several challenges we see facing thermochronology today, which could be important in the next forty years of the fields' evolution.

In general one of the greatest needs in thermochronology is better quantitative understanding of the kinetics of diffusion (and annealing), especially from experimental approaches. There are many important limitations to our understanding of Ar and He diffusion in many phases, and not nearly as many attempts to resolve these issues by direct experiments as there are applications with heuristic assumptions and attempted empirical "calibrations". Particularly important in this regard would be development of routine ways of measuring kinetic data directly on unknowns, rather than assuming all samples are the same, as is done for many types of minerals. Kinetic variations among specimens of the same mineral and strategic exploitation of these properties in sampling and analyses may in fact lead to great

advances in understanding kinetic mechanisms and controls in general, not to mention more detailed and accurate thermal histories. A related challenge that is more specific to (U-Th)/He dating is the need for agreed-upon, cost-effective, and reliable protocols for treating alpha-ejection and U-Th zonation on grain-by-grain bases.

Much thermochronologic interpretation assumes that daughter nuclides diffuse simply across zero-concentration grain boundaries into an infinite-sink reservoir. Whereas this idealized model has allowed a great deal of progress in interpreting noble gas thermochronometry, there are some natural examples that could be interpreted as evidence for violations of this behavior. Better theoretical and experimental understanding of the phenomena of excess Ar and He like those of Baxter (2003) may improve the robustness of thermochronologic interpretations in some cases. A better quantitative understanding of these issues may in fact provide important thermochronologic interpretations in unexpected areas (e.g., Kelley and Wartho 2001).

Another issue is the inherent uncertainty involved in inferring exhumational histories from thermal histories. One of the reasons for increasing interest in thermochronology in the last decade is the prospect of bringing radioisotopic dating techniques to bear on near-surface crustal processes, especially those constraining erosional exhumation. Even if the thermal histories themselves bore no uncertainty, inferring exhumation histories from them requires assumptions about geothermal gradients and their variations in space and time. These assumptions and their uncertainty range widely in complexity depending on the problem being addressed, but often involve spatial and temporal transients in exhumation rates, topography, fluid circulation, and deep-derived (basal) heat flow. Some of the currently most exciting issues such as evolution of paleotopography and erosion rates on 10^5-10^6 yr scales may rely on assumptions that are difficult to test or require extensive integration of other data sets such as heat flow or hydrologic data to constrain models. In many cases, convincing arguments can be made that the essential aspects of interpretations are insensitive to some of these assumptions. But in others, uncertainties such as how groundwater circulation patterns affect the thermal field at depths less than 2–3 km (especially in regions of high topographic relief, e.g., Ehlers 2005), or how magmatic events that may produce little surface expression affect thermal fields to greater depths, are difficult to constrain. At least some of these issues may be addressed by focused high-density sampling of currently active orogens, structures, or topographic features. If groundwater flow significantly deflects isotherms in the uppermost 2–3 km of high relief areas, for example, a careful heat-flow, hydrologic, and thermochronologic study could illuminate the details. Non-uniqueness in interpretations is not new to the Earth sciences, and thermochronologists and modelers can address uncertainties in interpretations by reporting the range of processes and solutions that satisfy a set of observations rather than looking for a single solution.

A general issue facing thermochronology is the problem of nonmonotonic thermal histories. It is generally acknowledged that while most datasets do not uniquely constrain model thermal histories, when data from enough different systems or high-quality multi-domain or closure profile data are available, a range of thermal histories emerges that is commonly sufficiently small to be geologically useful. It may be generally underappreciated, however, that many models often focus on solutions assuming monotonic cooling. When nonmonotonic cooling histories are allowed, it is often more difficult to find a family of thermal histories with a restricted enough range to be useful (e.g., Quidelleur et al. 1997; McDougall and Harrison 1999; Lovera et al. 2002). This is explicitly recognized in most formal inversions of fission-track age and length data, as well as multi-domain $^{40}Ar/^{39}Ar$ K-feldspar cooling models, but many casual users fail to recognize the importance or limitations of this assumption. Thermal histories from multiple thermochronometers with certain shapes (e.g., concave down, followed by concave up) may be consistent with simplified expectations of reheating, but they are not diagnostic (e.g., Harrison et al. 1979). In this respect, fission-track dating bears a distinct advantage

over noble gas methods, because track-length analysis allows resolution of distinct thermal histories for tracks for different ages. Nonetheless, realistic modeling of age and track-length data for thermal histories involving reheating is often subject to considerable uncertainty (e.g., Ketcham 2003, 2005). Ultimately, geologic considerations may provide critically important information in considering non-monotonic thermal histories, but development of techniques for diagnosing reheating from thermochronologic data alone may be an important goal for future studies. One potential tack may be to use contrasting responses of thermochronometers with strongly varying activation energies. Extremely short duration (1–100 yr) and relatively high temperature reheating events, for example, can produce diagnostic age inversions in fission-track and (U-Th)/He ages in the same minerals, because of their distinct kinetics.

Finally, compared with some disciplines in geophysics and geodesy (e.g., IRIS or UNAVCO), the thermochronological community is not particularly cohesive at the moment and there has been little formal effort to improve shared resources or improve the access to thermochronological data. There are considerable historical reasons for the current culture of each thermochronologist having their own facility and their own protocols. However, we suggest that the time may have come to consider development of a community-wide vision for sharing facilities to help support and encourage comprehensive regional studies. As we outlined earlier and as is discussed elsewhere in this volume (e.g., Ehlers 2005), the demand for large datasets will increase, given intellectual developments driven by modeling, the growing focus on low-temperature systems much affected by complex high-frequency boundary conditions (Braun 2005), intense interest in detrital thermochronology, and analytical demands stemming from community initiatives like Earthscope's USArrray and the Plate Boundary Observatory. These sorts of demands may completely overwhelm the capabilities of a single laboratory, and both cooperative work among laboratories and development of new high-throughput facilities will be required. We suggest that thermochronologists might benefit from pursuing a grander vision. There are important problems in geodynamics that could be solvable given high-enough sampling densities that, while a far stretch for current analytical capacity, are not economically out of reach, even today—investigators are often successful in procuring funds for seismic lines costing millions of dollars, a sum that could support tens of thousands of mineral ages, even using current systems not optimized for analytical throughput.

The future of thermochronology is bright. Intense interest in understanding near-surface processes and links between tectonics, erosion, and climate will continue to motivate advances in a number of areas that should increase the resolution and accuracy of thermochronologic models. New thermochronometeric systems are being developed that will expand accessible temperature ranges, better models of crystal-scale kinetic processes are clarifying age and thermal history interpretations, and analytical innovations will likely soon permit generation of large datasets that can invert for thermal histories of entire drainage basins or orogens, or provide routine closure profiles in single crystals. Improved geodynamic and surface process models will also undoubtedly allow increasingly sophisticated interpretations of tectonogeomorphic evolution. Motivated by exciting problems linking geologic processes such as tectonics, erosion, and climate, the next few decades will undoubtedly witness ingenious innovations and development of powerful analytical, interpretational, and modeling approaches that rival the progress and changes in radioisotopic dating in the last hundred years.

REFERENCES

Armstrong RL (1966) K-Ar dating of plutonic and volcanic rocks in orogenic belts. *In*: Potassium-Argon Dating. Schaeffer OA, Zähringer J (eds) Springer–Verlag, Berlin, p 117-133

Barfod GH, Frei R, Krogstad EJ (2002) The closure temperature of the Lu-Hf isotopic system in apatite. Geochim Cosmochim Acta 66:15A:51

Batt GM, Brandon M, Farley K, Roden-Tice M (2001) Tectonic synthesis of the Olympic Mountains segment of the Cascadia wedge, using two-dimensional thermal and kinematic modeling of thermochronological ages. J Geophys Res 106:26731-26746

Batt G, Braun J (1997) On the thermomechanical evolution of compressional orogens, Geophys J Int 128: 364-382

Baxter EF (2003) Quantification of the factors controlling the presence of excess ^{40}Ar or ^{4}He. Earth Planet Sci Lett 216:619-634

Baxter EF, DePaolo DJ, Renne PR (2002) Spatially correlated anomalous $^{40}Ar/^{39}Ar$ 'Age' variations about a lithologic contact near Simplon Pass, Switzerland: a mechanistic explanation for excess Ar. Geochim Cosmochim Acta 66:1067-1083

Beaumont CR, Jamieson RA, Nguyen MH, Lee B (2001) Himalayan tectonics explained by extrusion of a low-viscosity crustal channel coupled to focused surface denudation. Nature 414:738-742

Benfield A (1949) The effect of uplift and denudation on underground temperatures. J Appl Phys 20:66-70

Berger GW (1975) $^{40}Ar^{39}Ar$ step heating of thermally overprinted biotites, hornblendes and potassium feldspars from Eldora, Colorado. Earth Planet Sci Lett 26:387-408

Berger GW, York D (1981) Geothermometry from $^{40}Ar^{39}Ar$ dating experiments. Geochim Cosmochim Acta 45:795-811

Brandon MT, Roden-Tice MK, Garver JI (1998) Late Cenozoic exhumation of the Cascadia accretionary wedge in the Olympic Mountains, northwest Washington State. Geol Soc Am Bull 110:985-1009

Brandon MT, Vance JA (1992) Tectonic evolution of the Cenozoic Olympic Subduction Complex, Washington State, as deduced from fission-track ages for detrital zircons. Am J Sci 292:565-636

Braun J (2005) Quantitative constraints on the rate of landform evolution derived from low-temperature thermochrohonology. Rev Mineral Geochem 58:351-374

Braun J, Robert X (2005) Constraints on the rate of post-orogenic erosional decay from low-temperature thermochronological data: application to the Dabie Shan, China. Earth Surf Proc Land, in press

Braun J, Sambridge M (1997) Modelling landscape evolution on geological time scales; a new method based on irregular spatial discretization. Basin Res 9:27-52

Bullard EC (1938) The disturbance of the temperature gradient in the Earth's crust by inequalities of height. Monthly Notices Roy Astro Soc, Geophys Suppl 4:360-362

Calk LC, Naeser CW (1973) The thermal effect of a basalt intrusion on fission-tracks in quartz monzonite. J Geol 81:189-198

Cerveny PF, Naeser ND, Zeitler PK, Naeser CW, Johnson NM (1988) History of uplift and relief of the Himalaya over the past 18 Ma–Evidence from fission-track ages of detrital zircons from sandstones of the Siwalik Group. *In*: New Perspectives in Basin Analysis, Kleinspehn K, Paola C (ed) Univ. Minnesota Press, p. 43-61

Chamberlain KR, Bowring SA (2001) Apatite–feldspar U–Pb thermochronometer: a reliable, mid-range (~450 °C), diffusion-controlled system. Chem Geol 172:173-200

Cherniak DJ (1993) Lead diffusion in titanite and preliminary results on the effects of radiation damage on Pb transport. Chem Geol 110:177-194

Cherniak DJ, Watson EB (2001) Pb diffusion in zircon. Chem Geol 172:5-24

Cherniak DJ, Lanford WA, Ryerson FJ (1991) Lead diffusion in apatite and zircon using ion implantation and Rutherford Backscattering techniques. Geochim Cosmochim Acta 55:1663-1673

Cherniak DJ, Watson EB, Grove M, Harrison TM (2004) Pb diffusion in monazite: a combined RBS/SIMS study. Geochim Cosmochim Acta 68:829-840

Clark SP, Jäger E (1969) Denudation rate in the Alps from geochronologic and heat flow data. Am J Sci 267: 1143–1160

Coyle DA, Wagner GA (1998) Positioning the titanite fission-track partial annealing zone. Chem Geol 149: 117-125

Dahl PS (1996) The effects of composition on retentivity of argon and oxygen in hornblende and related amphiboles: A field-tested empirical model. Geochim Cosmochim Acta 60:3687-3700

Damon PE, Kulp JL (1957) Determination of radiogenic helium in zircon by stable isotope dilution technique. Transaction, Am Geophys Union 38:945-953

Dewey JF, Panhurst RP (1970) The evolution of the Scottish Caledonides in relation to their radiometric age patterns. Trans Royal Soc Edin 69:361-389

Dodson MH (1973) Closure temperature in cooling geochronological and petrological systems Contrib Mineral Petrol 40:259-274

Dodson MH (1979) Theory of cooling ages. *In:* Lectures in Isotope Geology. Jager E, Hunziker JC (eds.) Springer-Verlag, Berlin, p. 194

Dodson MH (1986) Closure profiles in cooling systems. *In:* Materials Science Forum, Vol 7, Trans Tech Publications, Aedermannsdorf, Switzerland, p 145-153

Ducea MN, Ganguly J, Rosenberg EJ, Patchett PJ, Cheng W, Isachsen C (2003) Sm-Nd dating of spatially controlled domains of garnet single crystals; a new method of high-temperature thermochronology. Earth Planet Sci Lett 213:31-42

Ehlers TA (2005) Crustal thermal processes and the interpretation of thermochronometer data. Rev Mineral Geochem 58:315-350

Ehlers TA, Farley KA (2003) Apatite (U-Th)/He thermochronometry: methods and applications to problems in tectonic and surface processes. Earth Planet Sci Lett 206:1-14

Ehlers TA, Willett SD, Armstrong PA, Chapman DS (2003) Exhumation of the central Wasatch Mountains, Utah: 2. Thermokinematic model of exhumation, erosion, and thermochronometry interpretation. J Geophys Res 108:2173, doi:10.1029/2001JB001723.

Ellis MA, Densmore AL, Anderson RS (1999) Development of mountainous topography in the Basin and Ranges, USA. Basin Res 11: 21-41

Evernden JF, Curtis GH, Kistler RW, Obradovich J (1960) Argon diffusion in glauconite, microcline, sanidine, leucite and phlogopite. Am J Sci 258:583-604

Farley KA (2000) Helium diffusion from apatite: General behavior as illustrated by Durango fluorapatite. J Geophys Res 105:2903-2914

Farley KA (2002) (U-Th)/He dating: techniques, calibrations, and applications. Rev Mineral Geochem 47: 819-844

Farley KA, Stockli DF (2002) (U-Th)/He dating of phosphates: apatite, monazite, and xenotime. Rev Mineral Geochem 48:559-577

Farley KA, Wolf RA, Silver LT (1996) The effects of long alpha-stopping distances on (U-Th)/He ages. Geochim Cosmochim Acta 60:4223-4229

Fechtig H, Kalbitzer S (1966) The diffusion of argon in potassium-bearing solids. *In:* Potassium-Argon Dating. Schaeffer OA, Zähringer J (eds) Springer, New York, p 68-107

Fitzgerald JD, Harrison TM (1993) Argon diffusion domains in K-feldspars I: microstructures in MH-10. Contrib Mineral Petrol 113:367-380

Foland KA (1994) Argon diffusion in feldspars. *In:* Feldspars and Their Reactions. Parsons I (ed.), Kluwer, Dordrecht, p. 415-447

Garver JI, Brandon MT (1994) Erosional exhumation of the British Columbia coast ranges as determined from fission-track ages of detrital zircon from the Tofino basin, Olympic Peninsula, Washington. Geol Soc Am Bull 106:1398–1412

Gleadow AJW, Duddy IR, Lovering JF (1983) Fission track analysis: a new tool for the evaluation of thermal histories and hydrocarbon potential. Aust Petrol Explor Assoc J 23:93-102

Grove M, Harrison TM (1996) ^{40}Ar* diffusion in Fe-rich biotite. Am Mineral 81:940-951

Hames WE, Bowring SA (1994) An empirical evaluation of the argon diffusion geometry in muscovite. Earth Planet Sci Lett 124:161-167

Hanson GN Gast PW (1967) Kinetic studies in contact metamorphic zones. Geochim Cosmochim Acta 31: 1119-1153

Hanson GN, Simmons KR, Bence AE (1975) ^{40}Ar^{39}Ar spectrum ages for biotite, hornblende and muscovite in a contact metamorphic zone. Geochim Cosmochim Acta 39:1269-1277

Harrison TM (1981) Diffusion of ^{40}Ar in hornblende. Contrib Mineral Petrol 78:324-331

Harrison TM, Armstrong RL, Naeser, CW, Harakal JE (1979) Geochronology and thermal history of the Coast Plutonic Complex, near Prince Rupert, British Columbia. Can J Earth Sci 16:400-410

Harrison TM, Clarke GKC (1979) A model of the thermal effects of igneous intrusion and uplift as applied to Quottoon pluton, British Columbia. Can J Earth Sci 16: 411-420

Harrison TM, Duncan I, McDougall I (1985) Diffusion of ^{40}Ar in biotite: temperature, pressure and compositional effects. Geochim Cosmochim Acta 49:2461-2468

Harrison TM, Heizler MT, Lovera OM (1993) In vacuo crushing experiments and K-feldspar thermochronometry. Earth Planet Sci Lett 117:169-180

Harrison TM, Lovera OM, Heizler MT (1991) ^{40}Ar/^{39}Ar results for alkali feldspars containing diffusion domains with differing activation energy. Geochim Cosmochim Acta 55:1435-1448

Harrison TM, McDougall I (1980a) Investigations of an intrusive contact, northwest Nelson, New Zealand-I. Thermal, chronological, and isotopic constraints. Geochim Cosmochim Acta 44:1985-2003

Harrison TM, McDougall I (1980b) Investigations of an intrusive contact, northwest Nelson, New Zealand-II. Diffusion of radiogenic and excess ^{40}Ar in hornblende revealed by ^{40}Ar/^{39}Ar age spectrum analysis. Geochim Cosmochim Acta 44:2005-2020

Harrison TM, McDougall I (1981) Excess ^{40}Ar in metamorphic rocks from Broken hill, New South Wales: Implications for ^{40}Ar/^{39}Ar age spectra and the thermal history of the region. Earth Planet Sci Lett 55: 123-149

Harrison TM, McDougall I (1982) The thermal significance of potassium feldspar K-Ar ages inferred from ^{40}Ar/^{39}Ar age spectrum results. Geochim Cosmochim Acta 46:1811-1820

Harrison TM, Grove M, Lovera OM, Zeitler PK (2005) Continuous thermal histories from inversion of closure profiles. Rev Mineral Geochem 58:389-409

Harrison TM, Zeitler PK (2005) Fundamentals of noble gas thermochronometry. Rev Mineral Geochem 58: 123-149

Harper CT (1967) The geological interpretation of potassium-argon ages of metamorphic rocks from the Scottish Caledonides. Scottish J Geol 3:46-66

Hart SR (1964) The petrology and isotopic mineral age relations of a contact zone in the Front Range, Colorado. J Geol 72:493-525

Hess JC, Lippolt HJ, Gurbanov AG, Michalski I (1993) The cooling history of the late Pliocene Eldzhurtinskiy granite (Caucasus, Russia) and the thermochronological potential of grain-size/age relationships. Earth Planet Sci Lett 117:393-406

Hawkins DP, Bowring SA (1999) U-Pb monazite, xenotime and titanite geochronological constraints on the prograde to post-peak metamorphic thermal history of Paleoproterozoic migmatites from the Grand Canyon, Arizona. Contrib Mineral Petrol 134:150-169

Hodges K (2003) Geochronology and thermochronology in orogenic systems. *In:* Treatise on Geochemistry. Turekian KK, Holland HD (eds) Elsevier, p 263-292

Hodges K, Boyce J (2003) Laser-ablation (U-Th)/He geochronology. Eos, Trans, Am Geophys U 84(46), Fall Meeting Supplement, Abstract V22G-05

Hourigan JK, Reiners PW, Brandon MT (2005) U-Th zonation-dependent alpha-ejection in (U-Th)/He chronometry. Geochim Cosmochim Acta 69:3349-3365

House MA, Farley KA, Stockli D (2000) Helium chronometry of apatite and titanite using Nd-YAG laser heating. Earth Planet Sci Lett 183:365-368

Hurley PM (1954) The helium age method and the distribution and migration of helium in rocks. *In:* Nuclear Geology. Faul H (ed), Wiley & Sons, 301-329

Hurley PM, Hughes J, Pinsoons WH, Fairbairn HW (1962) Radiogenic argon and strontium diffusion parameters in biotite at low temperatures obtained from Alpine fault uplift in New Zealand. Geochim Cosmochim Acta 26:67-80

Jäger E, Niggli E, Wenk E (1967) Rb-Sr Alterbestimmungen an Glimmern der Zentralalpen. Beitrage Geol. Karte Schweiz 134:1-67

Jenkin GRT, Ellam RM, Rogers G, Stuart FM (2001) An investigation of closure temperature of the biotite Rb-Sr system: The importance of cation exchange. Geochim Cosmochim Acta 65:1141-1160

John BE, Foster DA, Murphy JM, Cheadle MJ, Baines AG, Fanning CM, Copeland P (2004) Determining the cooling history of in situ lower oceanic crust—Atlantis Bank, SW Indian Ridge. Earth Planet Sci Lett 222:145-160

Kelly SP (2002) K-Ar and Ar-Ar dating. Rev Mineral Geochem 47:785-818

Kelley SP, Arnaud NO, Turner SP (1994) High spatial resolution $^{40}Ar/^{39}Ar$ investigations using an ultra-violet laser probe extraction technique. Geochim Cosmochim Acta 58:3519-3525

Ketcham RA (2005) Forward and inverse modeling of low-temperature thermochronometry data. Rev Mineral Geochem 58:275-314

Kelley SP, Wartho J-A, (2000) Rapid Kimberlite Ascent and the Significance of Ar-Ar Ages in Xenolith Phlogopites. Science 289:609-611

Ketcham RA (2003) Effects of allowable complexity and multiple chronometers on thermal history inversion. Geochim Cosmochim Acta (Abs), 67(18), Supp. 1, A213.

Ketcham RA, Donelick RA, Carlson WD (1999) Variability of apatite fission-track annealing kinetics: III. extrapolation to geological time scales. Am Mineral 84:1235-1255.

Kirchner JR, Finkel RC, Riebe CS, Granger DE, Clayton JL, King JG, Megahan WF (2001) Mountain erosion over 10 yr, 10 k.y., and 10 m.y. time scales. Geology 29:591-594

Kohn BP, Belton D, Brown RW, Gleadow AJW, Green PF, Lovering JF (2003) Comment on: "Experimental evidence for the pressure dependence of fission track annealing in apatite" by A.S. Wendt et al. [Earth Planet. Sci. Lett. 201 (2002) 593–607]. Earth Planet Sci Lett 215:299-306

Laslett GM, Green PF, Duddy IR, Gleadow AJW (1987) Thermal annealing of fission tracks in apatite. 2. A quantitative analysis. Chem Geol 65:1-13

Lees CH (1910) On the isogeotherms under mountain ranges in radioactive districts. Proc Roy Soc 83:339-346

Lovera OM, Richter FM, Harrison TM (1991) Diffusion domains determined by ^{39}Ar release during step heating. J Geophys Res 96:2057-2069

Lovera OM, Richter FM, Harrison TM (1989) The $^{40}Ar/^{39}Ar$ geothermometry for slowly cooled samples having a distribution of diffusion domain sizes. J Geophys Res 94:17917-17935

Lovera OM, Grove M, Harrison TM, Mahon KI (1997) Systematic analysis of K-feldspar $^{40}Ar/^{39}Ar$ step heating results: I. Significance of activation energy determinations. Geochim Cosmochim Acta 61:3171-3192

Lovera OM, Grove M, Harrison TM (2002) Systematic analysis of K-feldspar $^{40}Ar/^{39}Ar$ step heating results II: Relevance of laboratory argon diffusion properties to nature. Geochim Cosmochim Acta 66:1237-1255

Lovera OM, Heizler MT, Harrison TM (1993) Argon diffusion domains in K-feldspar II: Kinetic properties of MH-10. Contrib Mineral Petrol 113:381-393

McDougall I, Harrison TM (1999) Geochronology and Thermochronology by the $^{40}Ar/^{39}Ar$ Method. 2nd ed., Oxford University Press, New York

Mason B (1961) Potassium-argon ages of metamorphic rocks and granites from Westland, New Zealand. New Zealand J Geol Geophys 4:352-356

Mancktelow N, Grasemann B (1997) Time-dependent effects of heat advection and topography on cooling histories during erosion. Tectonophys 270:167-195

Mitchell SG, Reiners PW (2003) Influence of wildfires on apatite and zircon (U-Th)/He ages. Geology 31: 1025-1028

Musset AE (1960) Diffusion measurements and the potassium-argon method of dating. Geophys J Royal Astronom Soc 18:257-303

Naeser CW (1967) The use of apatite and sphene for fission track age determinations. Bull Geol Soc Am 78: 1523-1526

Naeser CW, Faul H (1969) Fission track annealing in apatite and sphene. J Geophys Res 74:705-710

Naeser CW, Forbes RB (1976) Variation of fission-track ages with depth in two deep drill holes. EOS Trans Am Geophys Union 57:353

Nasdala L, Reiners PW, Garver JI, Kennedy AK, Stern RA, Balan E, Wirth R (2004) Incomplete retention of radiation damage in zircon from Sri Lanka. Am Mineral 89:219-231

Parrish RR (1985) Some cautions which should be exercised when interpreting fission-track and other dates with regard to uplift rate calculations. Nucl Tracks 10:425

Parsons I, Brown WL, Smith JV (1999) $^{40}Ar/^{39}Ar$ thermochronology using alkali feldspars: real thermal history or mathematical mirage of microtexture?. Contrib Mineral Petrol 136:92-110

Purdy JW, Jäger E (1976) K-Ar ages on rock-forming minerals from the Central Alps. Mem 1st Geol Min Univ Padova 30, 31 p.

Quidelleur Z, Grove M, Lovera OM, Harrison TM, Yin A, Ryerson FJ (1997) The thermal evolution and slip history of the Renbu Zedong Thrust, southeastern Tibet. J Geophys Res 102:2659-2679

Rahl JM, Reiners PW, Campbell IH, Nicolescu S, Allen CM (2003) Combined single-grain (U-Th)/He and U/Pb dating of detrital zircons from the Navajo Sandstone, Utah. Geology 31:761-764

Rahn MK, Grasemann B (1999) Fission track and numerical thermal modeling of differential exhumation of the Glarus thrust plane (Switzerland). Earth Planet Sci Lett 169:245-259

Rahn MK, Brandon MT, Batt GE, Garver JI (2004) A zero-damage model for fission-track annealing in zircon. Am Mineral 89:473-484

Reiners PW (2005) Zircon (U-Th)/He thermochronometry. Rev Mineral Geochem 58:151-179

Reiners PW, Campbell IH, Nicolescu S, Allen CM, Hourigan JK, Garver JI, Mattinson JM, Cowan DS (2005) (U-Th)/(He-Pb) double dating of detrital zircons. Am J Sci 305:259-311

Reiners PW, Campbell IH, Nicolescu S, Allen CA, Hourigan JK, Garver JI, Mattinson JM, Cowan DS (2005) (U-Th)/(He-Pb) "double-dating" of detrital zircons. Am J Sci 305:259-311

Reiners PW, Farley KA (1999) He diffusion and (U-Th)/He thermochronometry of titanite. Geochim Cosmochim Acta 63:3845-3859

Reiners PW, Farley KA (2001) Influence of crystal size on apatite (U-Th)/He thermochronology: an example from the Bighorn Mountains, Wyoming. Earth Planet Sci Lett 188:413-420

Reiners PW, Spell TL, Nicolescu S, Zanetti KA (2004) Zircon (U-Th)/He thermochronometry: He diffusion and comparisons with $^{40}Ar/^{39}Ar$ dating. Geochim Cosmochim Acta 68:1857-1887

Richter FM, Lovera OM, Harrison TM, Copeland P (1991) Tibetan tectonics from $^{40}Ar/^{39}Ar$ analysis of a single K-feldspar sample Earth Planet Sci Lett 105:266-278

Robbins GA (1972) Radiogenic argon diffusion in muscovite under hydrothermal conditions. M.S. Thesis, Brown University. Providence, Rhode Island

Rutherford E (1905) Present problems in radioactivity. Pop Sci Monthly (May):1-34

Rutherford E (1906) Radioactive Transformations. Charles Scribner's Sons, NY

Scherer EE, Cameron KL, Blichert-Toft J (2000) Lu-Hf garnet geochronology; closure temperature relative to the Sm-Nd system and the effects of trace mineral inclusions. Geochim Cosmochim Acta 64:3413-3432

Shuster DL, Farley KA (2003) $^4He/^3He$ thermochronometry. Earth Planet Sci Lett 217:1-17

Shuster DL, Farley KA (2005) $^4He/^3He$ thermochronometry: theory, practice, and potential complications. Rev Mineral Geochem 58:181-203

Shuster DL, Farley KA, Sisterson JM, Burnett DS (2003) Quantifying the diffusion kinetics and spatial distributions of radiogenic ^4He in minerals containing proton-induced ^3He. Earth Planet Sci Lett 217: 19-32

Shuster DL, Vasconcelos PM, Heim JA, Farley KA (2005) Weathering geochronology by (U-Th)/He dating of goethite. Geochim Cosmochim Acta 69:659-673

Stock GM, Anderson RS, Finkel RC (2004) Pace of landscape evolution in the Sierra Nevada, California, revealed by cosmogenic dating of cave sediments. Geology 32:193-196

Stockli DF (2005) Application of low-temperature thermochronometry to extensional tectonic settings. Rev Mineral Geochem 58:411-448

Stuwe KL, White L, Brown R (1994) The influence of eroding topography on steady-state isotherms; application to fission track analysis. Earth Planet Sci Lett 124:63-7

Tagami T, Galbraith RF, Yamada R, Laslett GM (1998) Revised annealing kinetcs of fission tracks in zircon and geological implications In Van den haute P, De Corte F (eds) Advances in fission-track geochronology. Kluwer academic publishers, Dordrecht, The Netherlands, p 99-112

Vance D, Bickle M, Ivy-Ochs S, Kubik PW (2003) Erosion and exhumation in the Himalaya from cosmogenic isotope inventories of river sediments. Earth Planet Sci Lett 206:273-288

Vasconcelos PM (1999) K-Ar and $^{40}Ar/^{39}Ar$ geochronology of weathering processes. Ann Rev Earth Planet Sci 27:183-229

Vidal O, Wendt AS, Chadderton LT (2003) Further discussion on the pressure dependence of fission track annealing in apatite: reply to the critical comment of Kohn et al. Earth Planet Sci Lett 215:307-316

Villa IM (1994) Multipath Ar transport in K-feldspar deduced from isothermal heating experiments. Earth Planet Sci Lett 122:393-401

Wagner GA (1968) Fission track dating of apatites. Earth Planet Sci Lett 4:411–415

Wagner GA, Miller DS, Jäger E (1979) Fission-track ages on apatite of Bergell rocks from Central Alps and Bergell boulders in Oligocene sediments. Earth Planet Sci Lett 45:355-360

Wagner GA, Reimer GM, Jäger E (1977) Cooling ages derived from apatite fission track, mica Rb-Sr and K-Ar dating: The uplift and cooling history of the Central Alps. Mem Instit Geol Mn Univ Padova 30:1-27

Watt S, Durrani SA (1985) Thermal stability of fission tracks in apatite and sphene: Using confined-track-length measurements. Nuclear Tracks 10:349-357

Wendt AS, Vidal O, Chadderton LT (2002) Experimental evidence for the pressure dependence of fission track annealing in apatite. Earth Planet Sci Lett 201:593-607

Westcott MR (1966) Loss of argon from biotite in a thermal metamorphism. Nature 210:84-84

Wolf RA, Farley KA, Silver LT (1996) Helium diffusion and low-temperature thermochronometry of apatite. Geochim Cosmochim Acta 60:4231-4240

Wolf RA, Farley KA, Kass DM (1998) Modeling of the temperature sensitivity of the apatite (U-Th)/He thermochronometer. Chem Geol 148:105-114

Zeitler PK, Herczeg AL, McDougall I, Honda M (1987) U-Th-He dating of apatite: a potential thermochronometer. Geochim Cosmochim Acta 51:2865-2868

Zeitler PK (1987) Argon diffusion in partially outgassed alkali-feldspars: insights from $^{40}Ar/^{39}Ar$ analysis. Chem Geol (Isotope Geoscience Section) 65:167-181

Zeitler PK, Johnson NM, Briggs ND, Naeser CW (1986) Uplift history of the NW Himalaya as recorded by fission-track ages on detrital Siwalik zircons. *In:* Proceedings of the Symposium on Mesozoic and Cenozoic Geology in Connection of the 60th Anniversary of the Geological Society of China. Jiqing H. (ed) Geological Publishing House, Beijing, p. 481-494

Reviews in Mineralogy & Geochemistry
Vol. 58, pp. 19-47, 2005

Fundamentals of Fission-Track Thermochronology

Takahiro Tagami
Division of Earth and Planetary Sciences
Graduate School of Science
Kyoto University
Kyoto 606-8502, Japan
tagami@kueps.kyoto-u.ac.jp

Paul B. O'Sullivan
Apatite to Zircon, Inc.
1075 Matson Road
Viola, Idaho 83872-9709, U.S.A.
osullivan@apatite.com

INTRODUCTION

Fission-track (FT) analysis has developed into one of the most useful techniques used throughout the geologic community to reconstruct the low-temperature thermal history of rocks over geological time. The FT method is based on the accumulation of narrow damage trails (i.e., fission tracks) in uranium-rich mineral grains (e.g., apatite, zircon, titanite) and natural glasses, which form as a result of spontaneous nuclear fission decay of ^{238}U in nature (Price and Walker 1963; Fleischer et al. 1975). The time elapsed since fission tracks began to accumulate is estimated by determining the density of accumulated tracks in a particular material in relation to the uranium content of that material. Chemical etching can be used to enlarge fission tracks that have formed within a mineral in order to make them readily observable under an ordinary optical microscope (Price and Walker 1962).

If a host rock is subjected to elevated temperatures, fission tracks that have formed up to that point in time are shortened progressively and eventually erased by the thermal recovery (i.e., annealing) of the damage (Fleischer et al. 1975). Because thermal diffusion basically governs the annealing process, the reduction in FT length is a function of heating time and temperature. Importantly, fission tracks are partially annealed over different temperature intervals within different minerals. This characteristic allows for the construction of time-temperature paths of many different rock types by (a) plotting FT (and other isotopic) ages from different minerals versus their closure temperatures, which is applicable in the case of a monotonous cooling history (e.g., Wagner et al. 1977; Zeilter et al. 1982), and/or by (b) the inverse modeling of observed FT age and confined track length data (e.g., Corrigan 1991; Lutz and Omar 1991; Gallagher 1995; Ketcham et al. 2000; see also Ketcham 2005).

Fleischer et al. (1975) summarized the early studies of the solid-state nuclear track detection and its geological applications. Subsequently, a comprehensive overview of FT dating and thermochronology was provided by Wagner and Van den haute (1992), followed by more recent advances of the FT method in a number of review articles by Ravenhurst and Donelick (1992), Gallagher et al. (1998), Dumitru (2000), and Gleadow et al. (2002).

The aim of this particular chapter is to present a simplified and historical overview of some of the basic fundamentals of FT thermochronology, and is not written in an attempt to supersede

1529-6466/05/0058-0002$05.00 DOI: 10.2138/rmg.2005.58.2

all or any of the detailed review articles. This overview is designed to assist a reader of this volume in gaining a better understanding of some of the fundamentals of FT thermochronology prior to reading in-depth discussions of the apatite fission track (AFT) and zircon fission track (ZFT) methods, which are the focus of the following two chapters. Furthermore, there is bound to be some overlap between the content presented within this chapter and that within the following chapters discussing the AFT and ZFT methods. The authors have attempted to minimize this overlap wherever possible, however, readers should once again view this chapter as a historical overview of FT fundamentals, whereas the following chapters discuss some of the same fundamental ideas, but in much greater detail applicable to a particular technique.

FORMATION AND REGISTRATION OF NUCLEAR FISSION TRACKS

Spontaneous and induced nuclear fission decay

Nuclear fission is a process during which a heavy, unstable nucleus splits into a pair of fragments of similar size. This reaction takes place both spontaneously in nature and artificially during bombardment by neutrons and other high-energy particles or γ-rays. Each reaction is accompanied by the release of a few neutrons and ~210 MeV of energy, of which the majority (~170 MeV on average) is the kinetic energy of the fission fragments. As a result of this energetic disintegration, the fission fragments with massive positive charges are propelled from the reaction site in opposite directions. If the nucleus is located within a dielectric solid, the reaction will create a damage trail, called a fission track, along the trajectories of the two fragments.

Spontaneous fission occurs in very heavy nuclides that belong to the actinide series of elements. Of those nuclides, ^{232}Th and three U isotopes (^{234}U, ^{235}U and ^{238}U) are the typical candidates that produce a significant number of spontaneous fission tracks in solids. However, in regards to the relative abundances and spontaneous fission half-lives, ^{238}U is the only source of spontaneous tracks in terrestrial materials including natural apatite and zircon, except for those anomalously enriched in Th (Wagner and Van den haute 1992). Note that ^{238}U also decays through a chain comprised of eight α (^{4}He) and six β^- emissions. This decay, which occurs 2×10^6 times more frequently than the spontaneous fission events, needs to be taken into account in calculating an FT age. This will be discussed in more detail later.

Track formation process in solids

When a heavy ionized particle travels at a high velocity through a solid, it interacts with the host lattice, gradually loses its kinetic energy and slows down until it eventually stops. During this process, a couple of interactions are predominantly responsible for the deceleration of the particle: (1) electric interaction, more effective at high velocities, in which the particle surrenders its energy by stripping electrons from target atoms, by having its own electrons stripped away, and by raising the excitation level of the lattice electrons; and (2) nuclear interaction, more important as the particle slows down, in which the particle loses its energy by elastic collisions with lattice atoms. In addition, the energy is also partitioned to radiation (e.g., Chadderton 2003).

Although there is good agreement on the deceleration process of the charged particle and induced interactions, the debate has raged as to which mechanism causes the resultant motion of the lattice atoms that forms and registers the damage trails (e.g. Fleischer et al. 1975; Durrani and Bull 1987; Wagner and Van den haute 1992; Gleadow et al. 2002; Chadderton 2003). One of the widely accepted theories is the "ion explosion spike" model (Fleischer et al. 1965a, 1975) that treats electrostatic displacements as the primary process. In this model, track formation occurs during three stages (Fig. 1): (1) the rapidly moving positively-charged particle strips lattice electrons along its trajectory, leaving an array of positively-ionized lattice atoms; (2) the

resulting clusters of positive ions are displaced from their original lattice sites as a result of Coulomb repulsion, creating interstitials and vacancies; and (3) the stressed region relaxes elastically, straining the surrounding undamaged lattice. The creation of the long-ranged strains in the third stage makes possible the direct observation of unetched (or latent) tracks by transmission electron microscopy (TEM). This model explains the primary observation that particle tracks are observed only in dielectric solids having electric resistivity >2000 Ωm (Fleischer et al. 1975).

An alternative is the "thermal spike" model (Seitz 1949; Bonfiglioli et al. 1961; Chadderton and Montagu-Pollock 1963), in which the passage of an energetic particle is assumed to produce instantaneous, intense heating of the lattice along the trajectory. The track core is rapidly heated to a high temperature and subsequently quenched by thermal conduction into the surrounding lattice. As a result, lattice defects are created by the thermal activation and the track core is left disordered. Chadderton (2003) argued that both ion explosion and thermal spikes could be present to different degrees for track formation and registration in a variety of solids.

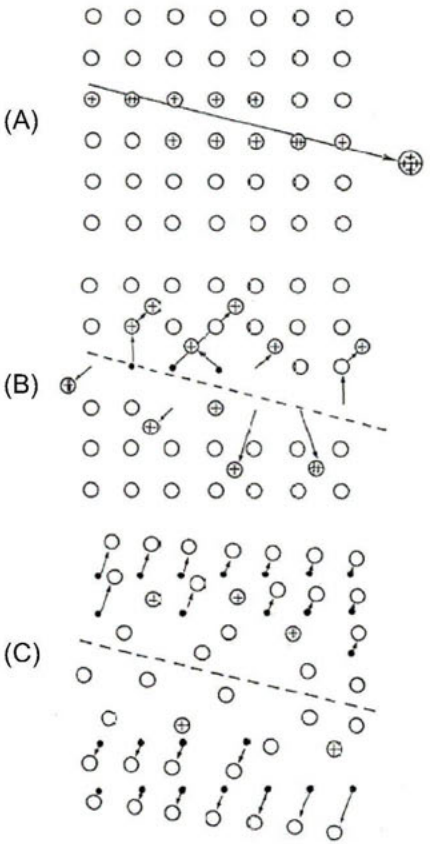

Figure 1. Formation and registration process of charged particle tracks in a dielectric solid by the ion explosion spike model (Fleischer et al. 1965a), which involves three stages: (A) the rapidly moving positively-charged particle strips lattice electrons along its trajectory, leaving an array of positively-ionized lattice atoms; (B) the resulting clusters of positive ions are displaced from their original lattice sites as a result of Coulomb repulsion, creating interstitials and vacancies; and (C) the stressed region relaxes elastically, straining the surrounding undamaged lattice.

Structure of the latent track

Knowledge on the structure of fission tracks in their latent state is critical not only to unravel their formation process but also to serve as a physical basis for their thermal annealing behaviors, which have conventionally been observed and quantified after chemical etching. Since the pioneering work by Silk and Barnes (1959), the atomic-scale characterization of latent tracks has been conducted using TEM and other analytical techniques on apatite (Paul and Fitzgerald 1992; Paul 1993), zircon (Yada et al. 1981, 1987; Bursill and Braunshausen 1990), muscovite mica (Thibaudau et al. 1991; Vetter et al. 1998) and other dielectric materials (see overviews by Fleischer et al. 1975; Wagner and Van den haute 1992; Neumann 2000; Chadderton 2003) (Fig. 2). In general, latent tracks represent a cylindrical shape of amorphous material in a crystalline matrix, with a sharp amorphous-crystalline transition. The elastic strain field around the disordered core extends a short distance into the matrix, likely with $1/R^2$ dependence (Bursill and Braunshausen 1990; R, radial distance), with no evidence for structural defects in its vicinity. The cross section of the track has a nearly circular shape with widths of 6–10 nm in apatite (Paul 1993), ~8 nm in zircon (Bursill and Braunshausen 1990) and ~4–10 nm in muscovite mica, depending on the ion energy loss (Vetter et al. 1998). The track is a linear, continuous feature and has approximately

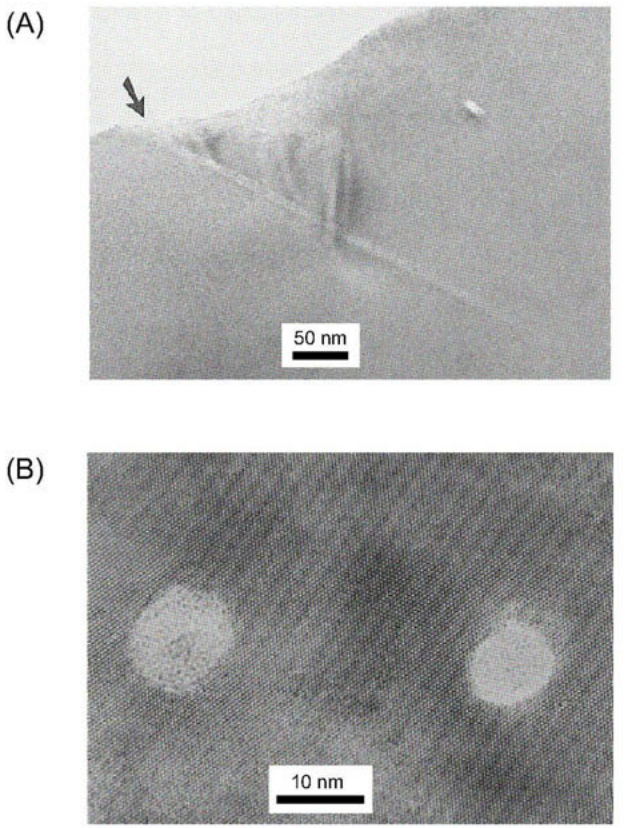

Figure 2. Atomic-scale images of latent (unetched) tracks: (A) an induced track in Durango fluorapatite observed subparallel to its length by transmission electron microscopy (Paul and Fitzgerald 1992) and (B) intersections of Pb ion tracks in muscovite mica imaged by 400 kV high-resolution transmission electron microscopy (Vetter et al. 1998).

a uniform diameter along most of its length. For its entire range, however, the track is a cylinder over a certain length and has a tapering-down in diameter near its end (Dunlap et al. 1997; Chadderton 2003), which may be the case of both terminals of a fission track (Carlson 1990).

The axial variation in damage density is deduced from a theoretical consideration on the rate of kinetic energy loss along a trajectory of nuclear fission fragments (Green et al. 1988; Wagner and Van den haute 1992). Since the kinetic energies of a pair of fission fragments are both below the Bragg peak in the energy loss curve, both fragments are most intensely ionizing, and therefore create most intensive damages, in the early part of their passage through the crystal lattice, i.e., around the site of the nuclear fission. As they slow down and lose energy, the damage intensity falls off away from this point, with the result that the damage density along the track peaks around the center and falls to zero at each end (Green et al. 1988).

CHEMICAL ETCHING AND OPTICAL MICROSCOPE OBSERVATION

Latent fission tracks can be viewed only by TEM and other high-resolution microscopic techniques because of their limited widths of only several nm. They, however, are conveniently

scanned only when samples have very high track densities (i.e., > 10^{10}cm^{-2}), which is generally not the case of terrestrial minerals such as apatite and zircon. Another potential problem with viewing latent fission tracks is that the entire range of each track cannot be observed at such a high magnification, despite the necessity to analyze track lengths for the modern FT thermochronometry method (Paul 1993). In this regard, a technique is needed to enlarge fission tracks in order to be visible at a lower magnification under an optical microscope. Of the visualization techniques available, by far the most general and widely used has been chemical etching, which utilizes the preferential chemical attack along the entire length of the fission tracks.

Basic process of track etching

Fission tracks can be enlarged by chemical etching because the disordered region of the track core is more rapidly dissolved than the surrounding undamaged bulk material, due to its lowered binding energy. Chemical etching is conducted by immersing a dielectric material into a particular reagent under strictly controlled temperature and time conditions. Thus, only tracks that intersect the material's surface are etched and enlarged for observation. The reagent and etching conditions are selected on an empirical basis and have been established for a variety of minerals and other dielectric solids (Fleischer et al. 1975; Durrani and Bull 1987; Wagner and Van den haute 1992).

The geometry of an etched track is controlled by the simultaneous action of two etching processes: chemical dissolution along the track at a rate V_T and general attack on the etched surface and on the internal surface of the etched track at a lesser rate V_G (Fleischer and Price 1963a,b) (Fig. 3). Under given etching conditions, V_T in general increases with ionization rate and thus varies along a track, whereas V_G is generally constant for a given material but can depend on crystallographic orientations. In natural glasses, which are typically amorphous, V_T is only a few times higher than V_G and hence the etched tracks appear as rounded cones. In crystals, however, V_T is generally much higher than V_G by more than a factor of 10 and this results in a needle-like track shape (Fig. 4). In the course of such etching, dissolution and removal of the latent track core is completed before the track is sufficiently enlarged and becomes visible under the optical microscope. Therefore, the visible enlargement process is predominantly governed by the progressive widening of the track channel to ~1 μm at a rate V_G. See previous literature for more details (Fleischer et al. 1975; Durrani and Bull 1987; Wagner and Van den haute 1992).

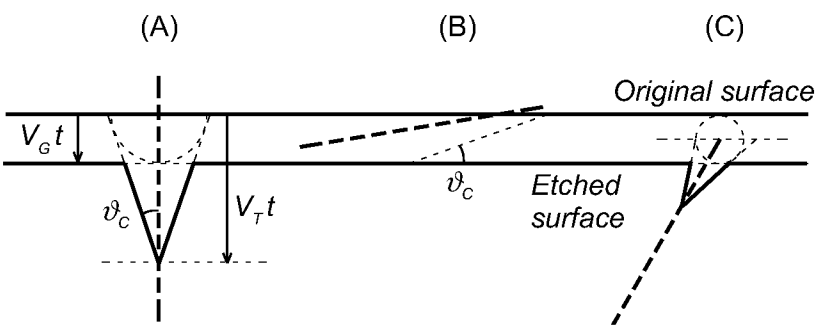

Figure 3. (A) The geometry of an etched track is controlled by two etching processes, i.e., chemical dissolution along the track at a rate V_T and general attack on the etched surface and on the internal surface of the etched track at a lesser rate V_G (Fleischer and Price 1963a,b): (B) Tracks inclined at relatively low angles to a surface (i.e., less than the critical angle, ϑ_C) are not etched to be observable under optical microscope: (C) New tracks that began and ended beneath the original surface are revealed by progressive removal of the surface itself. Here V_G/V_T is given as 1/3 throughout.

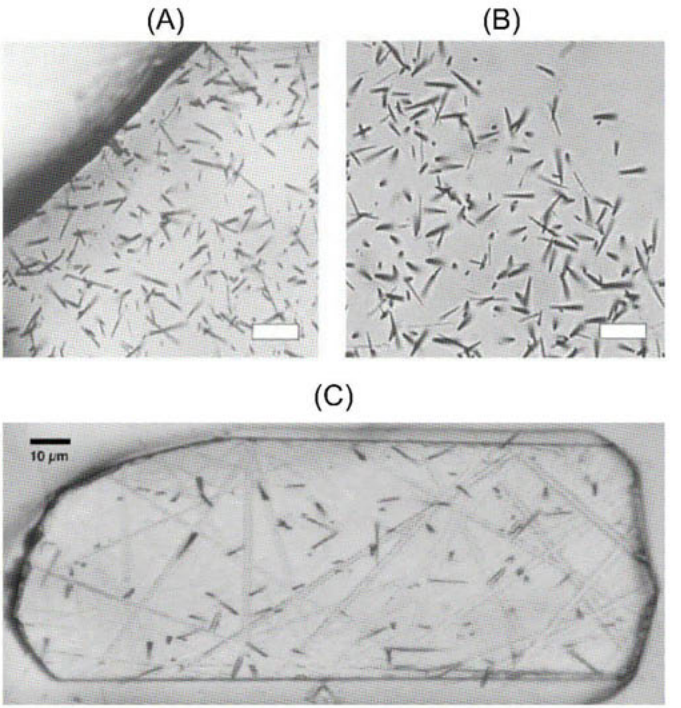

Figure 4. Photographs of etched fission tracks viewed under optical microscope. (A) Spontaneous tracks revealed on a polished internal surface of ~27.8 Ma Fish Canyon Tuff zircon. The crystallographic *c*-axis lies approximately vertical. (B) Induced tracks implanted on a muscovite detector (Brazilian Ruby clear) that were derived from the region of the photograph (A). (Photos by TT) (C) Spontaneous tracks on a polished internal surface of ~33 Ma apatite crystal. The *c*-axis lies approximately horizontal. (Photo by POS) Scale bars are 10 μm.

Etching efficiency and prolonged-etching factor

Because the surface of the mineral grain or glass is attacked and progressively removed during etching, tracks inclined at relatively low angles to the original surface are etched away. Such low-angle tracks are therefore not observable under the optical microscope (Fig. 3), which results in the number of latent tracks intersecting a given surface no longer being equal to that of etched ones on the surface. The minimum angle to the surface above which tracks are etched is called the critical angle ϑ_C, which is equal to arcsine (V_G/V_T) (Fleischer and Price 1964; Fleischer et al. 1975). An etching efficiency η is defined by the fraction of tracks intersecting a surface that are etched on the surface, and is given by $\cos^2\vartheta_C$ for the case of internal "thick" sources, where particle tracks originate throughout the volume of the detector itself. Thus:

$$\rho_E \equiv \eta\rho_L = \rho_L \cos^2\vartheta_C = \rho_L\left(1-\frac{V_G^{\,2}}{V_T^{\,2}}\right) \tag{1}$$

where ρ_E and ρ_L are the areal density of etched and latent tracks, respectively. ϑ_C can be experimentally determined by the etch-test of particle tracks that are implanted by the bombardment of collimated heavy ions at a certain angle to the sample's surface. Such experiments yielded ϑ_C values of ~25–35° for natural glasses and < 10° for crystals (Khan and Durrani 1972).

When tracks originating from the internal source are etched, new tracks that began and ended beneath the original surface are revealed by progressive removal of the surface itself (Fig. 3). As a result, the total number of tracks will increase monotonically as etching proceeds because the tracks etched at an early stage continue to be visible even after long etch times, although they grow and become less distinct. This effect is called the "prolonged-etching factor" (Kahn and Durrani 1972) and is quantified by:

$$\Delta\rho = N_F h\left(1-\sin\vartheta_C\right) \tag{2}$$

where $\Delta\rho$ is the areal density of new tracks added, N_F is a number of tracks per unit volume and h is the thickness of the layer removed. Because $\rho_L = gN_F R_L$, where g is a geometry factor of the detector (0.5 and 1 for external and internal surfaces, respectively) and R_L is an etchable range (i.e., length) of the latent track, thus:

$$\Delta\rho = \rho_L \frac{h\left(1-\sin\vartheta_C\right)}{gR_L} = \rho_E \frac{h}{gR_L\left(1+\sin\vartheta_C\right)} \tag{3}$$

Since $h = V_G t$, where t is a time duration of etching:

$$\Delta\rho = \rho_L \frac{V_G t\left(1-{V_G}/{V_T}\right)}{gR_L} \tag{4}$$

The total observed density of etched tracks ρ_O is thus given by:

$$\rho_O = \rho_E + \Delta\rho = \rho_L\left\{1-\frac{V_G^{\,2}}{V_T^{\,2}}+V_G t\frac{\left(1-{V_G}/{V_T}\right)}{gR_L}\right\} \tag{5}$$

Etching criteria and their influences on the observed track density and length

For reliable track density determination, the observed track density ρ_O needs to be as close to the latent track density ρ_L as possible. It is therefore desirable to analyze material that has lower V_G, so that ρ_E and $\Delta\rho$ come close to ρ_L and 0, respectively. Because V_G is anisotropic in crystals, it is necessary to employ a crystal surface having the lowest V_G. This is particularly important with highly anisotropic minerals, such as zircon and sphene (Fig. 5). A conventional way to identify surfaces of low V_G is to check whether the etched surface has clear and sharp polishing scratches that indicate relatively low $V_G t$ (Naeser et al. 1980;

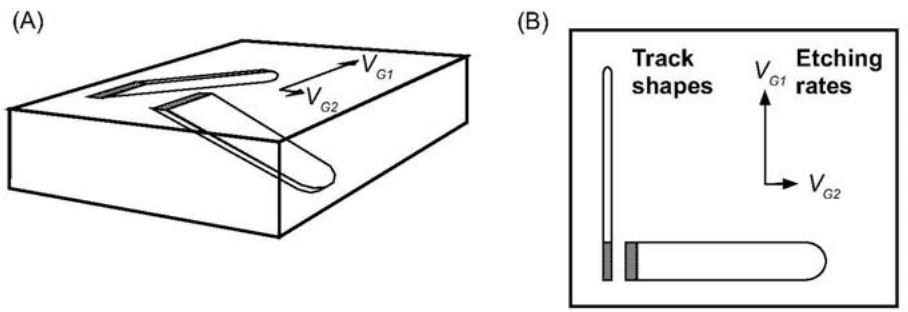

Figure 5. (A) Shape of etched tracks in minerals having highly anisotropic V_G (i.e., a big contrast between V_{G1} and V_{G2}). (B) Top view of the etched mineral surface, on which track revelation is also highly anisotropic. After Gleadow (1981).

Gleadow 1981). Secondly, etch time t needs to be as short as possible to minimize $\Delta\rho$. Thus, in theory, etching should be stopped when all tracks that intersect the original surface become clearly visible under the optical microscope. Because V_G changes between individual samples, particularly zircon and sphene, the optimum etch time must be determined by the step-etch and observation procedure (Gleadow 1981; Hasebe et al. 1994).

Care should be taken when etching minerals having highly anisotropic V_G, on which track revelation is also anisotropic. That is, tracks lying subparallel to a certain crystallographic orientation (e.g., c-axis in case of zircon) are more slowly enlarged than others because they have lower rates of widening of the track channel due to lower V_G perpendicular to the track orientation (Gleadow 1981). For such samples, track etching should be continued until the tracks that are etched most slowly and weakly become visible under the microscope, so that the number of etched tracks is approximately equal for all crystallographic orientations (Gleadow 1981; Sumii et al. 1987). Otherwise, ρ_O will be grossly underestimated relative to ρ_L. Further complexity and difficulty is due to the fact that the V_G anisotropy is not constant between samples but shows a systematic decrease as a result of accumulation of radiation damages. Hence, special care is needed to etch young zircons and sphenes because they have higher anisotropy due to the low level of radiation damage and because for such samples, ρ_L is in general so low that it is often difficult to judge the optimum etching condition using a small number of tracks therein (Gleadow 1980; Watanabe 1988).

The observed range (i.e., length) of etched track, R_E, is also different from R_L, the etchable range of the latent track, due primarily to the outer growth of the track channel as the etching proceeds (Fig. 6). As the overestimation of the range, ΔR, is approximately given by $\Delta R = 2V_G t$ (Laslett et al. 1984), thus:

$$R_E \equiv R_L + \Delta R = R_L + 2V_G t \qquad (6)$$

If V_G is isotropic and $V_T >> V_G$, the width of etched track, W_E, is approximately equal to $2V_G t$ and is accordingly a good measure of ΔR. In the case of crystals, however, V_G is generally anisotropic and W_E merely offers a rough estimate of ΔR. For an ordinary etching condition, $\Delta R \approx W_E = \sim 1$ μm and therefore is not negligible for confined track length analysis that will be mentioned later. Since ΔR is a function of t and increases as the etching proceeds, standardization of etching condition is required for reliable track length measurement as well as for inter-laboratory comparison of length data.

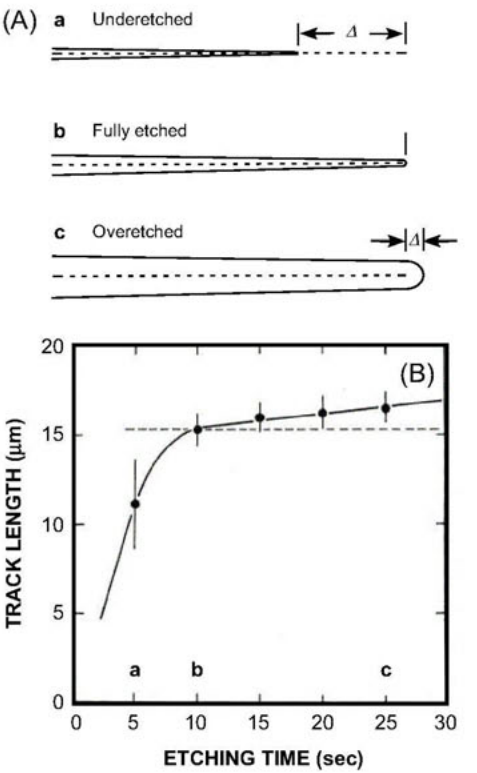

Figure 6. (A) Three stages of track revelation and associated errors (Δ) of the observed track length in apatite. The dot line represents an unetched (latent) track. (B) Observed track length vs. total etching time. Note the steady increase in the observed length after being fully etched, due primarily to the outer growth of the track channel as the etching proceeds. After Laslett et al. (1984).

DERIVATION OF AGE CALCULATION EQUATION

In principle, a radiometric age is given by three parameters, i.e., the numbers of parent and daughter nuclides in a material, and the decay constant for the parent nuclide. In the FT method, they are respectively the number of ^{238}U per unit volume, ^{238}N, the number of spontaneous fission tracks per unit volume, N_S, and the decay constant for spontaneous nuclear fission, λ_F. Because ^{238}U also decays by α-emission with a much greater decay constant (1.55125×10^{-10}y^{-1}), λ_D, the basic formula for a FT age, t, is given by:

$$N_S = \frac{\lambda_F}{\lambda_D} {}^{238}N\left\{\exp(\lambda_D t) - 1\right\} \tag{7}$$

To measure ^{238}N, the nuclear fission reaction of ^{235}U that is artificially induced by thermal neutron irradiation is utilized. The number of induced fission tracks per unit volume, N_I, is given by:

$$N_I = {}^{235}N\sigma_F\Phi \tag{8}$$

where ^{235}N is the number of ^{235}U per unit volume, σ_F is the cross section for induced nuclear fission of ^{235}U by thermal neutrons (580.2×10^{-24}cm^2), and Φ is the thermal neutron fluence. From these equations,

$$t = \frac{1}{\lambda_D} \ln\left\{1 + \left(\frac{\lambda_D}{\lambda_F}\right)\left(\frac{N_S}{N_I}\right) I\sigma_F\Phi\right\} \tag{9}$$

where I is the isotopic abundance of U, $^{235}N/^{238}N$ (7.2527×10^{-3}). Only tracks intersecting the etched surface are observable under an optical microscope and thus:

$$t = \frac{1}{\lambda_D} \ln\left\{1 + \left(\frac{\lambda_D}{\lambda_F}\right)\left(\frac{\rho_S}{\rho_I}\right) QGI\sigma_F\Phi\right\} \tag{10}$$

where ρ_S is the surface density of etched spontaneous fission tracks, ρ_I is the surface density of etched induced fission tracks, Q is the integrated factor of registration and observation efficiency of fission tracks, and G is the integrated geometry factor of etched surface. In this equation, λ_F is not well determined (Bigazzi 1981; Van den haute et al. 1998), whereas Q and Φ are generally difficult to measure accurately (Van den haute et al. 1998). Although, in principle, it is possible to determine these constants and values individually and calculate t absolutely (Wagner and Van den haute 1992; Van den haute et al. 1998), the empirical zeta calibration based on the analysis of age standards (Hurford and Green 1982, 1983; see also Fleischer et al. 1975) was recommended by the IUGS subcommission on Geochronology (Hurford 1990) and has since been used universally. Φ is conventionally measured by the induced fission-track density on a U-doped standard glass, ρ_D, irradiated together with the sample, and is thus given by:

$$\Phi = B\rho_D \tag{11}$$

where B is a calibration constant empirically determined. Thus, the zeta age calibration factor, ζ, is defined accordingly by:

$$\zeta \equiv B\frac{I\sigma_F}{\lambda_F} \tag{12}$$

Hence,

$$t = \frac{1}{\lambda_D} \ln\left\{1 + \lambda_D\zeta\rho_D\left(\frac{\rho_S}{\rho_I}\right) QG\right\} \tag{13}$$

ζ is determined empirically by analyzing a set of standard materials of known ages (Hurford 1990). Q is the same between the age standards and age-unknown samples as long as they are analyzed using identical experimental procedures and criteria. In the routine analysis, therefore, Q is ignorable and ζ, is given by inputting the measured data of standard (i.e., ρ_D, ρ_S and ρ_I) and the reference age t into the equation above.

STABILITY AND FADING OF TRACKS

Basic process of track fading

Knowledge of the stability and fading of fission tracks is critically important in order to decode the geological history recorded by the host mineral. Of several possible environmental effects that could alter fission tracks, the most pervasive and recognized one is thermal annealing (Fleischer et al. 1975). The thermal annealing of fission tracks at increased temperature (or time) is a process during which the amorphous, disordered core is gradually restored to the ordered structure of crystalline matrix, as confirmed by TEM observation (Paul and Fitzgerald 1992; Paul 1993) (Fig. 7). The process is characterized by (1) the development of irregular morphology at the track-matrix boundary, (2) segmentation of the track, i.e., appearance of gaps, (3) an increase in the spacing between segments, the shape of which approaches a sphere, and (4) instantaneous healing of spheres, with an observable minimum diameter of ~3 nm (Paul 1993). The annealing likely occurs through the diffusion of interstitial atoms and lattice vacancies to recombine as a result of their thermal activation due to heating.

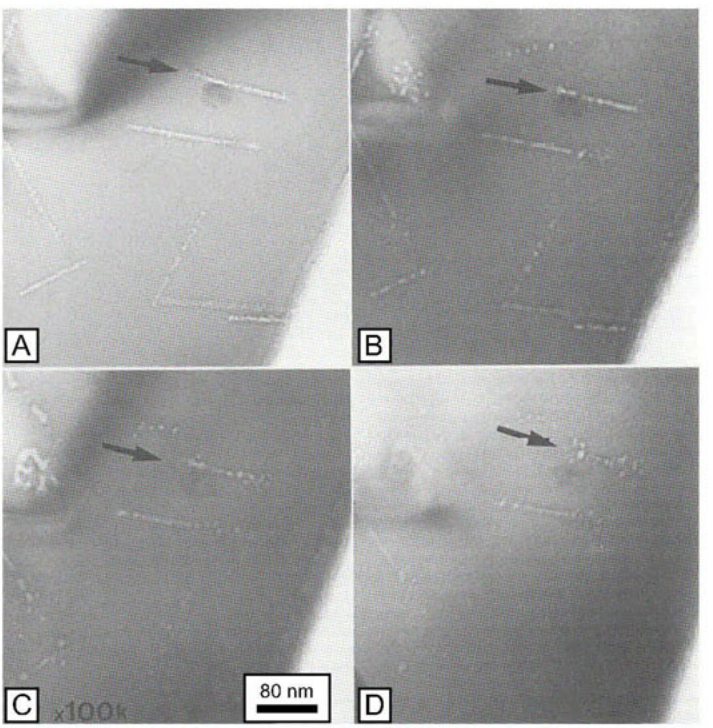

Figure 7. (A) – (D): Radiolytic-thermal annealing processes of induced tracks in Durango fluorapatite (after Paul and Fitzgerald 1992). The annealing proceeds from (A) to (D), as a consequence of electron-beam exposure and heating on the sample.

The thermal annealing behavior of fission tracks has been characterized and quantified using etched tracks, upon which routine thermochronologic studies are based. At the optical-microscopic scale, fission tracks progressively shrink from each end during early stages of annealing, as suggested by confined track-length analyses on apatite (Green et al. 1986; Donelick 1991; Donelick et al. 1999) and on zircon (Yamada et al. 1995a) (Fig. 8). At later stages of annealing, fission tracks continue to shrink, and appear to become broken into separate segments, with a result of a gross increase in standard deviation of track lengths for a specific crystallographic orientation (Green et al. 1986; Hejl 1995; Yamada et al. 1995a).

Track annealing at geological timescales: procedures and findings

Understanding the long-term annealing behaviors of the FT system over geological timescales is essential to unravel thermal histories of terrestrial and planetary materials. The conventional approach towards this is to: (1) make a systematic, quantitative description of FT annealing behaviors in laboratory under well-controlled conditions of temperature, time,

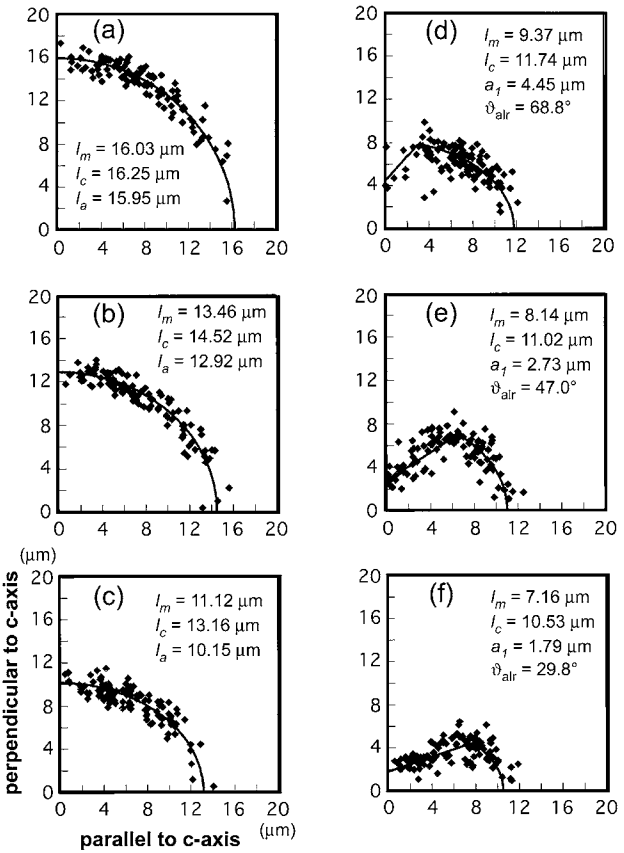

Figure 8. Polar coordinate plots of the induced fission-track lengths measured for Durango apatite at various degrees of annealing (Donelick et al. 1999). At relatively low degrees of annealing (a-c), fission-track lengths are approximately uniformly distributed about an ellipse with respect to track angle to the crystallographic *c*-axis. At higher degrees of annealing (d-f), the ellipse collapses, with fission tracks at relatively high angles to the crystallographic *c*-axis experiencing systematic, accelerated length reduction. As the degree of annealing increases, the initiation of the collapse of the ellipses rotates toward the *c*-axis.

pressure, etc., (2) predict FT annealing under plausible geological conditions by extrapolating a numerical annealing model constructed using the laboratory annealing data, (3) test the prediction by analyzing fission tracks in natural materials for which the thermal history and other environmental conditions are known or inferred with some confidence, and (4) modify and recalibrate the numerical annealing model, if necessary.

The long-term annealing characteristics of the FT system have been studied at a variety of natural settings; such as deep boreholes (e.g., Naeser and Forbes 1976; Gleadow and Duddy 1981; Green et al. 1989a; Corrigan 1993; Wagner et al. 1994; Tagami et al. 1996; Coyle and Wagner 1998; Hasebe et al. 2003) (Fig. 9), exposure of deeply buried sections (e.g., Zaun and Wagner 1985; Stockli et al. 2002), contact metamorphic aureoles (e.g., Naser and Faul 1969; Calk and Naeser 1973; Tagami and Shimada 1996), regional diagenetic and metamorphic zones (e.g., Green et al. 1996; Brix et al. 2002), monotonous cooling of plutonic and metamorphic rocks (e.g., Harrison et al. 1979; Hurford 1986), etc.

Some important results discussed in the aforementioned natural annealing studies are briefly summarized below (details will be discussed in following chapters):

- In geologic studies, even those involving thermally undisturbed volcanic rocks, the measured lengths of spontaneous tracks are not always equal to the measured lengths of induced tracks. Of note: length measurements are made on "confined" tracks (Laslett et al. 1982); i.e., tracks that are located within a crystal and are etched through a host track or cleavage, so that they exhibit their entire lengths (Fig. 10). For instance, confined track length data from apatite indicate that spontaneous tracks are always shorter than induced tracks (Wagner and Storzer 1970; Bertel et al. 1977; Green 1980; Gleadow et al. 1986), whereas this is not the case for zircon (Hasebe et al. 1994) and sphene (Gleadow 1978).
- FT annealing is indistinguishable between laboratory and nature in terms of the appearance and patterns of track shortening (Green et al. 1989a; Tagami and Shimada 1996), implying that the same physical processes consistently govern track annealing. This is also supported by the fact that the existence of fossil and modern

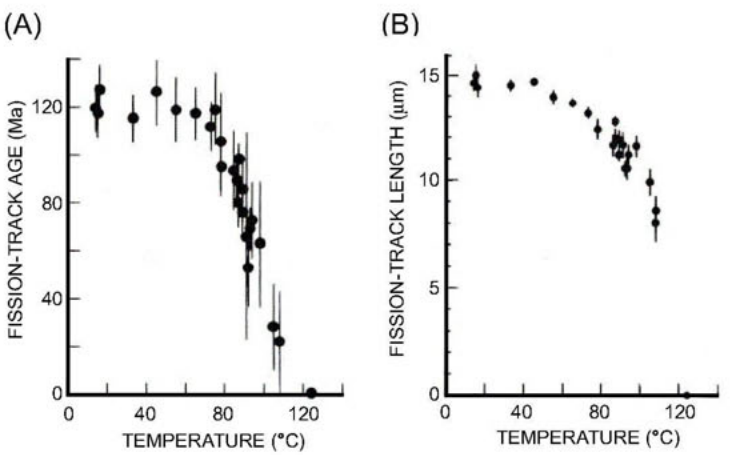

Figure 9. Long-term natural annealing of fission tracks in apatite observed in borehole samples from the Otway Basin, Australia, for which the geological evolution was well constrained (after Green et al. 1989a). Both fission-track age (A) and length (B) are reduced progressively down to zero in the temperature range of ~60–120 °C due to the increase in geothermal temperature with depth. Error bars are ± 2σ.

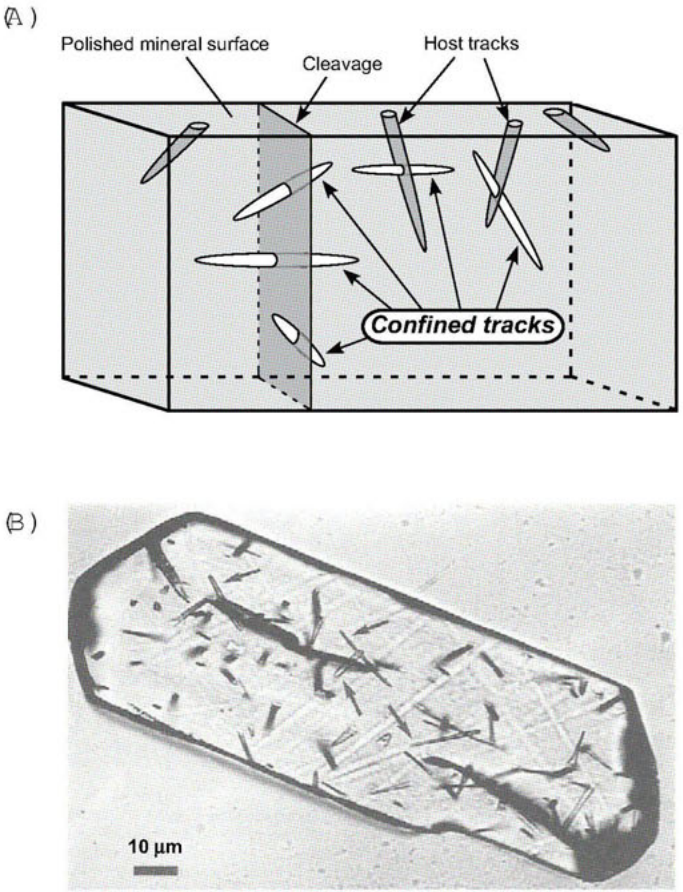

Figure 10. (A) A schematic illustration of an etched mineral that reveals confined tracks of different dimensions, i.e., tracks-in-cleavage (TINCLEs) or tracks-in-track (TINTs). (B) A top-view photograph of etched spontaneous tracks on a polished internal surface of apatite crystal (after Gleadow et al. 1986). Most of the visible tracks are surface-intersecting spontaneous tracks, which are used for age determination. Arrows point to four individual confined tracks (revealed as TINCLEs) exhibiting original entire track lengths, which are useful for estimating the true length distribution.

partial annealing zones (PAZ's; e.g., Fitzgerald and Gleadow 1990) was confirmed within a variety of geological settings (e.g., Calk and Naeser 1973; Naeser and Forbes 1976; Gleadow and Duddy 1981; Zaun and Wagner 1985; Green et al. 1989a; Corrigan 1993; Wagner et al. 1994; Tagami and Shimada 1996; Coyle and Wagner 1998; Stockli et al. 2002).

- Thermal sensitivities of fission tracks and other thermochronometers at geological timescales were inferred by relative positions of the PAZs (or partial retention zones), showing a reasonable consistency with the sensitivities observed in the laboratory (Calk and Naeser 1973; Coyle and Wagner 1998; Stockli et al. 2002; Reiners 2003; Tagami et al. 2003).
- The FT annealing behaviors predicted by extrapolating numerical annealing models have been tested on apatite (Green et al. 1989b; Corrigan 1993; Ketcham et al. 1999)

and on zircon (Tagami et al. 1998), with a result that the predictions are generally consistent with observations. However, at least in the case of apatite, this really only holds true when the mineral species being modeled is identical in composition to the mineral species for which the model was generated. This accordingly requires the use of a "multi-kinetic" model that theoretically incorporates both compositional and crystallographic effects (e.g., Ketcham et al. 1999).

Laboratory heating experiments: procedures and findings

Where laboratory-heating experiments are conducted on pieces of a material containing fission tracks at a series of temperatures (T), the time (t) to produce a given degree of annealing of the fission tracks was classically described by:

$$t = A \exp\left(\frac{E_A}{kT}\right) \tag{14}$$

where k is Boltzmann's constant, A is a constant and E_A is the activation energy (e.g., Naeser and Faul 1969; Fleischer et al. 1975). The degree of annealing is represented by iso-density or iso-length contours, when the data are displayed on a variation of an Arrhenius plot, i.e., the "$1/T$ vs. log t" diagram (Fig. 11). In earlier studies, the rate equation that describes FT annealing was given by first-order kinetics (e.g., Mark et al. 1973, 1981; Zimmermann and Gaines 1978; Bertagnolli et al. 1981; Huntsberger and Lerche 1987), in forms equivalent to:

$$\frac{dr}{dt} = -\alpha(T)r, \text{ with } \alpha(T) = \alpha_0 \exp\left(-\frac{E_A}{kT}\right) \tag{15}$$

where r is the degree of annealing, which is measured by the reduced FT density (or length) normalized to the unannealed value, and α_0 is a constant. This formulation is valid if the annealing results from diffusion of lattice defects having a unique E_A.

Later studies demonstrated, however, that the first-order kinetics gave a poor description of track annealing of minerals, such as apatite and zircon (e.g., Green et al. 1988; Green and Duddy 1989). Higher-order processes using a rate equation gave the more preferred description:

$$\frac{dr}{dt} = -\alpha(T)(1-r)^n \tag{16}$$

where n is approximately −3 to −4 for the Durango apatite (Laslett et al. 1987). Green et al. (1988) argued that, whereas the diffusive motion of individual disordered atoms may fundamentally be controlled by first-order kinetics, the annealing actually observed on etched fission tracks is a result of a number of complicated processes: i.e., the reduction in r is a manifestation of the reduction in atomic disorder that consists of a number of defects in an anisotropic, multi-component mineral.

Originally, laboratory heating experiments were aimed at determining the reduction in etched track density, upon which the FT dating method was based (e.g., Wagner 1968; Naeser and Faul 1969; Nagpaul et al. 1974; Bertel and Mark 1983). More recent studies, however, focused primarily on: 1) the reduction in length of etched tracks with which FT annealing is more precisely quantified, and 2) the distribution of etched confined track lengths, the shape of which is indicative of a rock's thermal history (e.g., Green et al. 1986; Carlson et al. 1989; Crowley et al. 1991; Donelick 1991; Yamada et al. 1995ab; Donelick et al. 1999; Barbarand et al. 2003ab). Here it is noted that the observed mean confined track length of spontaneous fission tracks in apatite and zircon grains separated from rapidly cooled and thermally undisturbed volcanic rocks is approximately constant (~14.5–15.0 μm for apatite; Gleadow et al. 1986; ~10.5 μm for zircon; Hasebe et al. 1994). Thus, these values offer good controls to measure length reduction of unknown samples.

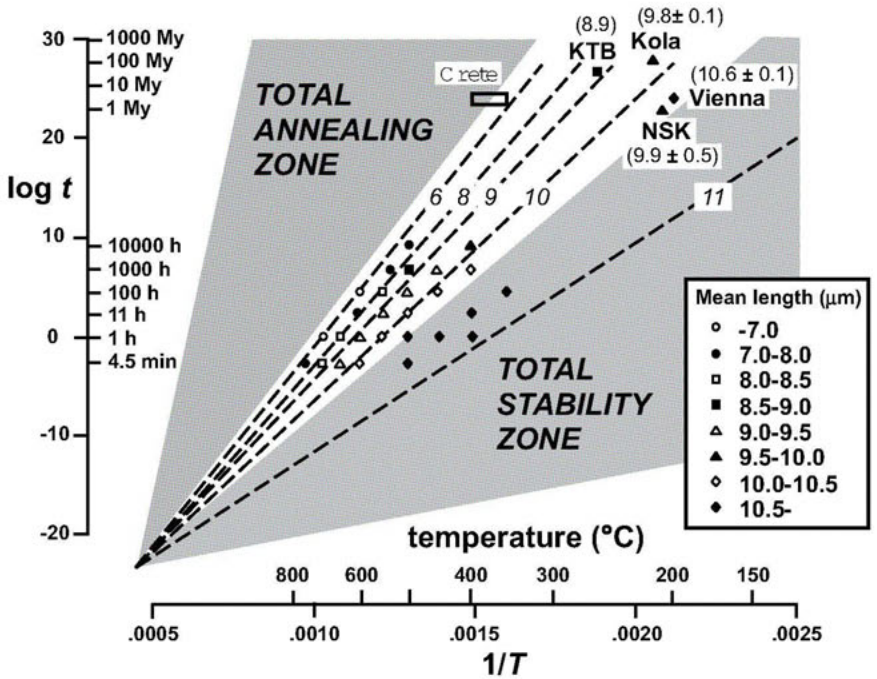

Figure 11. Arrhenius plot showing the design points of the laboratory annealing experiments of spontaneous fission tracks in zircon as well as contour lines for the fitted fanning model extrapolated to geological time scale (Yamada et al. 1995b; Tagami et al. 1998; model after Galbraith and Laslett 1997). Also shown are data points of four deep borehole samples subjected to long-term natural annealing, which were used to test the extrapolation of the annealing model (Tagami et al. 1998; Hasebe et al. 2003), and a box that indicates the time-temperature condition estimated for the higher temperature limit of the zircon PAZ on Crete (Brix et al. 2002). Three temperature zones can be defined as first-order approximation of fission-track annealing: the total stability zone (TSZ) where tracks are thermally stable and hence accumulated as time elapsed; the partial annealing zone (PAZ) where tracks are partially stable and slowly annealed and shortened; and the total annealing zone (TAZ) where tracks are unstable and faded soon after their formation. Note that the zircon PAZ is defined here as a zone having mean lengths of ~4 to 10.5 μm (Yamada et al. 1995b) and shown as a white region intervened by the TSZ and TAZ.

Heating experiments have typically been conducted under muffle-type or other electric furnaces, with samples being heated to varying temperatures under dry conditions, and pressures equal to one atmosphere. However, to assess the influence of various geological environmental factors, such as pressure, deformation, etc., a variety of heating systems and settings were employed during some tests, including the belt apparatus for dry and high-pressure conditions (Fleischer et al. 1965b), and the hydrothermal synthetic apparatus to synthesize hydrothermal-pressurized conditions (Wendt et al. 2002; Yamada et al. 2003). These experiments were usually carried out isochronally, i.e., at a set temperature with a variable time duration, or isothermally, for a controlled time duration with variable temperature. Once etched, fission tracks are no longer useful for further annealing runs because the chemical etching completely dissolves the damage core of latent tracks thus permanently preserving the etched track length. Therefore, each aliquot of a sample is annealed and analyzed for each step of heating experiments.

The results from numerous annealing experiments have previously been summarized by Fleischer et al. (1975), Durrani and Bull (1987), and Wagner and Van den haute (1992), and a similar scale of summarization is beyond the scope of this chapter. However, some

of the important results reported from these experiments, other than those mentioned in the last section, are briefly summarized below (some details will be discussed in the following chapters):

- The track annealing rate, dr/dt, depends upon the crystallographic orientation of the tracks. For instance, fission tracks parallel to the *c*-axis anneal at a slower rate than do those perpendicular to it for both apatite (Green et al. 1986; Donelick 1991; Donelick et al. 1999), and zircon (Tagami et al. 1990).
- The annealing rate also depends upon the chemical composition of a mineral, e.g., fission tracks in Cl-rich apatites anneal more slowly than do those in OH- and F-rich apatites (Green et al. 1986; Crowley et al. 1991; Carlson et al. 1999; Barbarand et al. 2003a).
- The annealing rate may depend upon the accumulation of radiation damage in crystals, such as zircon and sphene. Experimental data suggest that spontaneous fission tracks in older zircons (i.e., having greater damage accumulation) anneal slower than do those in young zircons (Kasuya and Naeser 1988; Carter 1990; Yamada et al. 1998; Rahn et al. 2004).
- The annealing rate possibly depends to some degree on pressure. While three studies using different experimental systems show no such dependence on the annealing rate in zircon (Fleischer et al. 1965b; Brix et al. 2002; Yamada et al. 2003), similar studies report conflicting results in terms of a pressure influence on apatite annealing (Wendt et al. 2002; Kohn et al. 2003; Donelick et al. 2003). See Donelick et al. (2005) for further discussion of this topic as it pertains to apatite.
- The use of different etchants can give rise to different track annealing rates: an example is HCl vs. NaOH etchants for sphene (Fleischer et al. 1975).
- Fission tracks in some materials undergo slow annealing at low ambient temperatures. For instance, extremely fresh fission tracks induced by thermal neutron bombardment in apatite show appreciable reduction in etchable length at temperatures < 23 °C (Donelick et al. 1990). This is consistent with the observation that unannealed spontaneous fission tracks are always shorter than unannealed induced fission tracks in apatite (Gleadow et al. 1986).
- The effects of various experimental biases are assessed in track length measurement of both unannealed and annealed fission tracks, which is indispensable for reliable interpretation of FT data (Green 1988; Galbraith et al. 1990; Yamada et al. 1995a; Donelick et al. 1999; Barbarand et al. 2003b).
- Numerical FT annealing models (i.e., kinetics) have been investigated and improved on apatite (Laslett et al. 1987; Carlson 1990; Crowley et al. 1991; Laslett and Galbraith 1996; Ketcham et al. 1999) and on zircon (Yamada et al. 1995b; Galbraith and Laslett 1997; Tagami et al. 1998), opening a way to the inverse modeling of geological thermal history (Crowley 1985, 1993; Green et al. 1989; Corrigan 1991; Lutz and Omar 1991; Gallagher 1995; Issler 1996; Willet 1997; Ketcham et al. 2000). See following chapters for more details (Donelick et al. 2005 on apatite kinetics; Tagami 2005 on zircon kinetics; Ketcham 2005 for inverse modeling).

EXPERIMENTAL PROCEDURES

Brief descriptions of individual experimental steps are given in this section, with a particular focus on the external detector method (EDM), the most widely accepted method of dating mineral grains at this time (Fig. 12). See previous discussions by Naeser (1976), Gleadow

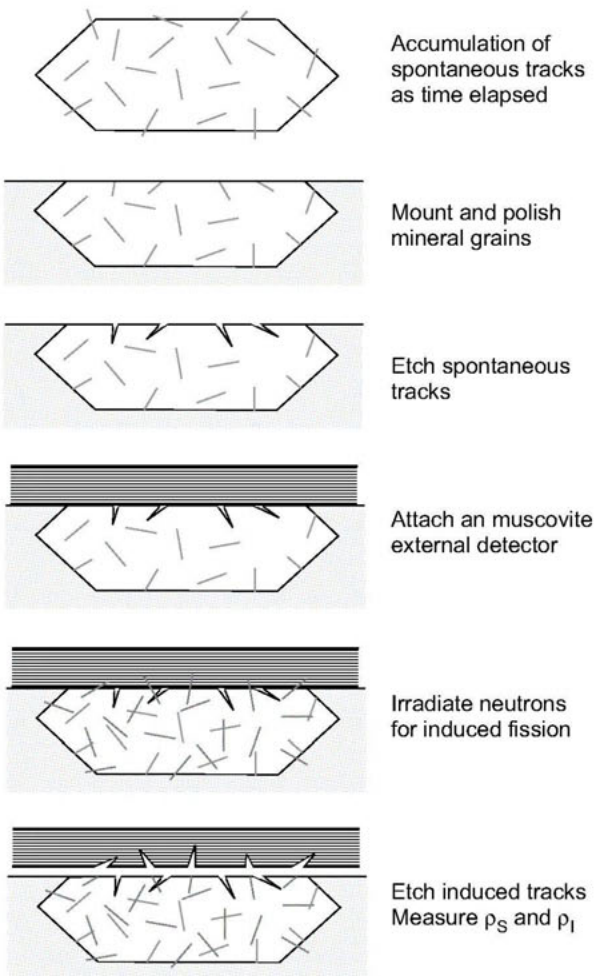

Figure 12. Schematic illustration of the experimental steps involved in the external detector method. The technique is by far the most popular dating procedure for mineral samples collected from a variety of geologic settings. ρ_S = surface density of etched spontaneous fission tracks; ρ_I = surface density of etched induced fission tracks.

(1984), Tagami et al. (1988), Ravenhurst and Donelick (1992), Wagner and Van den haute (1992) and Dumitru (2000) for further details as well as for other procedures and materials. See Donelick et al. (2005) for further discussion and suggestions of proposed experimental procedures as they pertain to apatite.

Methods of analysis

The FT age determination of an unknown sample is based upon the measurement of three different track densities, i.e., ρ_S, ρ_I and ρ_D. The first two densities are measured directly from the sample. At one time or another, a variety of experimental procedures have been employed in order to make these measurements, depending to some extent on the nature of the material to date (i.e., Naeser 1979; Gleadow 1981; Hurford and Green 1982; Ravenhurst and Donelick 1992; Wagner and Van den haute 1992).

Originally, the "population method" was the most popular for FT analysis of many different minerals, but is now recommended only for dating of glasses. In this procedure, ρ_S and ρ_I are both measured on the internal mineral surface using separate aliquots of the same sample. Induced fission tracks are etched and revealed on surfaces of mineral grains from which spontaneous fission tracks were removed by laboratory heating prior to the neutron irradiation. This procedure has the advantage that ρ_S and ρ_I are measured on surfaces of the same material that have identical track registration efficiencies. However, the disadvantage of this procedure is that FT ages cannot be measured on individual mineral grains. In addition, this procedure assumes that the two aliquots possess equal uranium concentrations and no zoning within individual grains, assumptions that need careful statistical and experimental assessments for individual samples.

At the time of publication of this chapter, by far the most widely used procedure is the external detector method (EDM) (Fig. 12). In this procedure, spontaneous fission tracks (ρ_S) are etched and revealed on an internal polished surface of a mineral grain, whereas induced fission tracks (ρ_I) are recorded on an external detector (e.g., thin sheet of a low-U muscovite mica) that is firmly attached onto the etched grain surface during neutron irradiation. Thus, ρ_S and ρ_I are measured respectively on the internal mineral surface and on the external detector surface. The advantage of this procedure is that FT ages can be determined on individual mineral grains, which is particularly important when attempting to date grains with varying ages and compositions within individual samples. Previous studies of both sedimentary rocks (e.g., Green et al. 1989a; Hurford and Carter 1991; Burtner et al. 1994; Barbarand et al. 2003a) as well as some basement rocks (O'Sullivan and Parrish 1995), have shown that significant variations in grain ages can occur within individual samples, and thus having the ability to date individual grains instead of simply determining a bulk sample age is imperative. The disadvantage is that because ρ_S and ρ_I are measured on different materials (i.e., original grain vs. mica detector), great care is needed to standardize etching conditions for each, particularly in the case of zircon and sphene that have variable and anisotropic etching characteristics (Gleadow 1978, 1981; Sumii et al. 1987). It is also noted that the sensitivity for track etching can be different between the mineral and external detector, as experimentally shown for apatite and zircon and muscovite detector (Iwano et al. 1992, 1993; Iwano and Danhara 1998). These points should be taken into account when applying an absolute age calibration (Wagner and Van den haute 1992; Van den haute et al. 1998), or when comparing observed zeta factors between different minerals or laboratories (Green 1985; Tagami 1987; Iwano and Danhara 1998).

Of special note, new procedure that utilizes a laser ablation ICP-MS to measure uranium values from individual grains, has recently been proposed (e.g., Cox et al. 2000; Hasebe et al. 2002, 2004; Svojtka and Kosler 2002; Kosler and Sylvester 2003), and may soon develop into the most widely recommended and utilized method. See Donelick et al. (2005) for further discussion on the use of laser ablation ICP-MS in FT age calculation and analysis of apatite.

Sample preparation and track etching

Minerals suitable for FT dating, such as apatite, zircon and sphene, are concentrated and separated from their host rock samples by conventional mineral separation techniques. The mineral grains are mounted into grain-holding materials, such as epoxy resin or a Teflon sheet (Gleadow et al. 1976; Naeser 1976; Ravenhurst and Donelick 1992). The sample mount is ground and polished to expose internal mineral surfaces (which should have at least $R/2$ distance to the original mineral surface for having 4π geometry). Spontaneous fission tracks that intersect the polished surface are revealed by placing the sample mount into an appropriate chemical reagent, such as acid or eutectic alkali (e.g., Fleischer et al. 1975), under particular time and temperature conditions. After etching, the sample is rinsed thoroughly to remove the reagent from the sample.

Neutron irradiation

An external detector, such as a thin low-uranium (<5 ppb) muscovite mica sheet, is firmly attached to each etched mineral mount. Individual sample-detector pairs are stacked between standard glass dosimeters, such as NIST-SRM 612 (or 962a) or Corning CN1 through CN6, on each of which the detector is also attached. The sample-standard stacks are then bombarded by neutrons at a well-thermalized irradiation facility in a nuclear reactor. Note that a substantial error is introduced in the age calculation if the sample is irradiated at a poorly-thermalized facility because induced fission tracks of the same size are also formed by epithermal- and fast-neutron induced fissions of ^{235}U as well as by fast-neutron induced fissions of ^{238}U and ^{232}Th (Crowley 1985; Tagami and Nishimura 1989, 1992). After irradiation and radioactive cooling, the muscovite detectors are detached from the samples, and are then etched to reveal tracks that were induced into the mica following decay of uranium within mineral grains during irradiation. See Green and Hurford (1984) and Wagner and Van den haute (1992) for more details of the neutron irradiation issue.

Track density determination

To determine ρ_S, ρ_I and ρ_D, the number of etched tracks that intersect the surface within a known area are counted using an optical microscope at magnifications of at least ~1000×. The following points need to be taken into account for reliable track density determination (e.g., Green 1981):

(1) Only mineral grains (or areas in individual grains) that satisfy the following criteria should be measured to determine ρ_S.

   (a) Grains should be free of spurious, non-track features, such as dislocations or tiny inclusions, and grains having many non-track features are best avoided. In many cases, however, non-track features are readily distinguishable from spontaneous fission tracks, which are straight, of limited length and randomly oriented.

   (b) Fission tracks on the grain surface should be well etched and clearly visible. This is particularly critical to dating zircon and sphene as they have, as mentioned above, variable and anisotropic etching characteristics (Gleadow 1978, 1981; Sumii et al. 1987).

   (c) Uranium distribution should be approximately homogeneous within the grain. This can generally be judged by variation in ρ_S on the grain surface. For samples of low ρ_S, variation in ρ_I on the muscovite detector will help.

(2) When using the EDM, ρ_S is counted on the etched internal surface of each mineral grain, whereas ρ_I is counted on the external detector surface within the corresponding area. Thus, for precise FT dating a reliable correlation is needed in order to move between the two areas.

Track length measurement

Analysis of horizontal confined tracks. As defined earlier, and shown in Figure 10, confined tracks are those contained entirely within the boundaries of the crystal being analyzed. For the purpose of measurement, these are etched to be observable with help of two primary types of host features having different geometries, known as Track-in-Track (TINT) and Track-in-Cleavage (TINCLE) (Lal et al. 1969). Laslett et al. (1982) documented that, of various length parameters, the greatest information about the true length distribution can be obtained from the measurement of "horizontal" confined tracks. This technique is by far the most popular approach to estimate the true length distribution of spontaneous fission tracks in minerals that is indispensable for quantitative modeling of rocks' thermal histories as well as for determining FT thermal annealing kinetics. The following points need to be taken into

account for reliable determination of confined track lengths (for further details, see Donelick et al. 2005 and Tagami 2005):

(1) Not only the length but also the crystallographic orientation should be measured for individual fission tracks because the track-annealing rate depends upon the crystallographic orientation.

(2) Only tracks having appropriate etched width should be measured because, as mentioned above, the observed FT length is a function of t and increases significantly as the etching proceeds. This is particularly enhanced when we analyze partially annealed samples that contain segmented tracks because the observed length of such tracks is very sensitive to the degree of etching (Green et al. 1986; Hejl 1995; Yamada et al. 1995a).

(3) While many FT analysts still measure TINCLE's in apatite in order to boost the number of confined track lengths measured for individual samples, it should be noted that natural etching of tracks does occur along pre-existing cracks or cleavage planes; thus, measuring TINCLE's can result in length distributions that are unrepresentative of the sample's true thermal history (Jonckheere and Wagner 2000).

Techniques to increase the number of measurable confined tracks. It is often difficult to measure sufficient number of confined tracks for reliable estimation of track length distributions when analyzing samples with low spontaneous track densities. To resolve this, three techniques have been developed to artificially increase the number of host tracks or cleavages that raises the probability of observing more confined tracks: 1) irradiation of nuclear fission fragments using the ^{252}Cf source (Donelick and Miller 1991), 2) irradiation of heavy nuclides using the accelerator (Watanabe et al. 1991) and 3) artificial fracturing using a well-controlled grinding machine (Yoshioka et al. 1994). See Yamada et al. (1998) for comparison of the three techniques in analyzing young zircons. See Donelick et al. (2005) for details and procedures for using a ^{252}Cf source for apatite and Tagami (2005) for procedures of artificial fracturing for zircon.

DATA ANALYSIS AND GRAPHICAL DISPLAYS

An analytical scheme for single-grain (or grain-by-grain) data obtained by the EDM is briefly presented below. See Wagner and Van den haute (1992) for data analysis of the population method. See Donelick et al. (2005) for a discussion of data analysis using the laser ablation ICP-MS.

Statistical test of single-grain data and error calculation of sample mean age

Routinely 10–30 single-grain ages are determined for a single FT analysis. If the grains within the sample have a common age, the variation in single grain ages is governed only by the Poissonian statistics concerned with the determination of ρ_S, ρ_I and ρ_D. In this case, ρ_S and ρ_I are obtained from:

$$\rho_S = \frac{\sum N_{Sj}}{\sum A_j} \qquad \rho_I = \frac{\sum N_{Ij}}{\sum A_j} \tag{17}$$

where N_{Sj} is the number of spontaneous fission tracks in area A_j of the j^{th} crystal and N_{Ij} is the number of induced fission tracks in the same area of the corresponding grain print on the muscovite detector (e.g., Green 1981). Then, the uncertainty in the mean age t is given by the formula:

$$\frac{\sigma(t)}{t} = \left(\frac{1}{N_S} + \frac{1}{N_I} + \frac{1}{N_D} \right)^{1/2} \tag{18}$$

where N_S, N_I and N_D are the total numbers of counted tracks for ρ_S, ρ_I and ρ_D, respectively. In reality, however, the assumption mentioned above is not necessarily valid for a number of factors (see Green 1981) and thus a statistical procedure, called χ^2-test (Galbraith 1981; see also Green 1981), was developed to assess the validity. It was shown that results from the conventional formula give the best estimate of (ρ_S/ρ_I) and $\sigma(\rho_S/\rho_I)$, as long as the observed track counts are acceptable under a χ^2-criterion:

$$\chi^2 = \sum \left\{ \frac{\left(N_{Sj} - P_{Sj}\right)^2}{P_{Sj}} \right\} + \sum \left\{ \frac{\left(N_{Ij} - P_{Ij}\right)^2}{P_{Ij}} \right\} \tag{19}$$

where $P_{Sj} = N_S(N_{Sj}+N_{Ij})/(N_S+N_I)$; $P_{Ij} = N_I(N_{Sj}+N_{Ij})/(N_S+N_I)$. Here the χ^2-value is tested at a desirable critical level, say 5%, with $(n-1)$ degree of freedom where n is the number of grains counted.

If the χ^2-value is unacceptable, it suggests that the data suffer from extra- Poissonian variation(s) due to a variety of experimental and geological factors (Burchart 1981; Green 1981), such as:

(a) incomplete revelation of spontaneous fission tracks, particularly in the case of zircon and sphene, which have more complex etching characteristics as mentioned above,

(b) imprecise track counting, particularly in the case of samples having high track densities or those having a great proportion of non-track features,

(c) incomplete contact between crystals and muscovite detectors,

(d) inhomogeneity of uranium within the measured grain,

(e) spatial variation of the thermal neutron flux on a scale of the areal distance of mounted grains (i.e., ~0.1 to 10 mm),

(f) inherent variability of single-grain ages in the sample dated, such as the case of reworked volcanic ash beds, sedimentary rocks having multiple detrital age components, and partially annealed samples with a significant variation in the thermal sensitivities among grains dated (e.g., apatites with a spread of Cl contents).

In the above cases, usage of conventional formula for the sample mean age and its uncertainty is no longer valid. Where the values of log (ρ_S/ρ_I) can be approximated by a Normal distribution, the central age and age dispersion will yield a better approximation of the population ages (Galbraith and Laslett 1993).

Graphical displays of single-grain age distribution

If the extra-Poissonian variation(s) are statistically detected in the single-grain age data, the structure of the spread in measured single-grain ages should be assessed in order to constrain the source of errors. For this, graphical methods have been employed using (a) the one-dimensional plot, or histogram, (b) the interval plot using, e.g., 95% confidence intervals (Seward and Rhoades 1986), (c) the age spectra, or weighted histogram (Hurford et al. 1984), and (d) the radial plot (Galbraith 1988, 1990) (Fig. 13). Of these, the most widely used today is the radial plot, in which the uncertainty in a single age estimate is isolated so that it is easier to judge the variation in ages between crystals. When multiple age populations are deduced in the radial plot of the sample data, statistical models can be applied to estimate the component ages, particularly the youngest age population (Galbraith and Green 1990; Brandon 1992; Galbraith

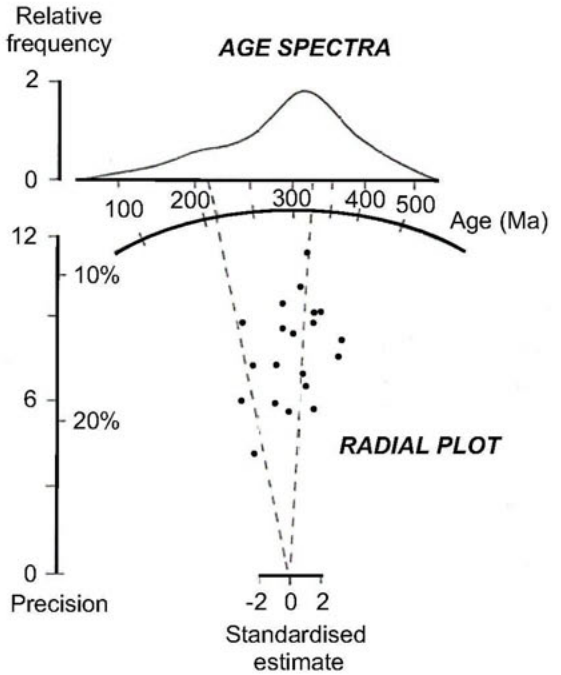

Figure 13. The age spectra (top) and radial plot (bottom) of twenty apatite grains from a sample artificially composed of two age groups (i.e., ~240 and ~340 Ma) (After Galbraith and Green 1990; Wagner and Van den haute 1992). The two dashed lines show the component age estimates. In the radial plot, the horizontal and vertical axes represent the standardized age estimate and reciprocal error, respectively.

and Laslett 1993) (Fig. 13). This technique is critical to the study of provenance ages using the detrital FT thermochronology (see Hurford and Carter 1991; Carter and Moss 1999; Garver et al. 1999; Ruiz et al. 2004) as well as to identify and extract the "essential age" in dating volcanic ash layers (e.g., Naeser et al. 1973; Gleadow 1980; Kowallis et al. 1986; Kohn et al. 1992; Andriessen et al. 1993; O'Sullivan et al. 2001), and even granitic rocks containing apatite grains with varying compositions (O'Sullivan and Parrish 1995).

Graphical displays of track length distribution

Approximately 50–100 confined tracks are routinely measured for each sample, even though even this number should be considered an absolute minimum. The distribution of track lengths is classically shown using a histogram with 1 μm bins since the general overall uncertainty of measured lengths is around 0.5 μm, due primarily to the outer growth of etched track channels as mentioned above. Because the track annealing is anisotropic, the angular distribution diagram is also used widely to rigorously judge the degree of partial annealing of tracks (Green et al. 1986; Donelick 1991; Ravenhurst and Donelick 1992; Yamada et al. 1995ab; Donelick et al. 1999; Barbarand et al. 2003b) (Fig. 8). In the case of apatite, mean track lengths either parallel or perpendicular to the *c*-axis can be used, instead of the usual mean track length, as fitted parameters of track annealing models (Carlson et al. 1999; Donelick et al. 1999; Ketcham et al. 1999). Mean track lengths for zircon are calculated using tracks ≥60° to *c*-axis so that the effects of anisotropic annealing and etching are minimized (Yamada et al. 1993, 1995ab).

The key issue in interpreting the observed length distribution is that longer tracks tend to be over-represented because they have a greater probability of being etched and observed as TINTs or TINCLEs than shorter tracks (Laslett et al. 1982) (Fig. 10). This sampling bias needs to be appropriately corrected to obtain the real length distribution, which is necessary

for the quantitative thermal history modeling of the observed FT data. In theory, the bias is proportional to the track length (Laslett et al. 1982) and this was empirically confirmed by the "two-component mixtures" experiment (Galbraith et al. 1990). In practice, however, other geometrical complexities will further be introduced into the track length analysis; i.e., the anisotropy in track etching and annealing for TINTs as well as the effective thickness of host fractures for TINCLEs (Galbraith et al. 1990). Furthermore, these factors can vary according to different experimental and analytical conditions/criteria used between laboratories as well as between observers (Barbarand et al. 2003; see also Yamada et al. 1995a). A proposed methodology to overcome much of this bias is described in further detail by Donelick et al. (2005).

CONCLUDING REMARKS

More than four decades have passed since Price and Walker (1963) first documented the possibility of FT dating, and more than two decades since the introduction of quantitative modeling of a rock's thermal history based upon the confined track length analysis of apatite (e.g., Laslett et al. 1982; Green et al. 1989a). Fission track thermochronology is now considered a mature method. Even so, it has recently been the subject of calibration and tuning towards more reliable reconstruction of thermal histories, as represented by the "multi-kinetic" thermal modeling (Carlson et al. 1999; Donelick et al. 1999; Ketcham et al. 1999). Furthermore, new lines of research are now emerging to potentially refine the technique further: (a) FT analysis of monazite (Gleadow et al. 2002, 2004; Fayon 2004), (b) FT analysis using laser ablation ICP-MS, with which one can potentially obtain both fission track and U/Pb ages on the same single crystal (Cox et al. 2000; Hasebe et al. 2002, 2004; Svojtka and Kosler 2002; Kosler and Sylvester 2003; Donelick et al. 2005), and (c) experimental characterization of very short-term track annealing using the graphite furnace, which simulates frictional heating of fault motions and thus may offer an innovative tool in the geo- and thermochronology of fault systems (Murakami et al. 2002; Murakami and Tagami 2004; Tagami 2005).

ACKNOWLEDGMENTS

We thank Barry Kohn and Diane Seward for their constructive reviews on the manuscript. TT has been supported by a Grant-in Aid (no. 12440137) as well as by a Grant-in-Aid for the 21st Century COE Program (Kyoto University, G3) from the Japanese Ministry of Education, Culture, Sports, Science and Technology.

REFERENCES

Andriessen PA, Helmes M, Hooghiemstra H, Riezebos PA, Van der Hammen T (1993) Absolute chronology of the Pliocene-Quaternary sediment sequence of the Bogota area, Colombia. Quatern Sci Rev 12:483-501

Barbarand J, Carter A, Wood I, Hurford AJ (2003a) Compositional and structural control of fission-track annealing in apatite. Chem Geol 198:107-137

Barbarand J, Hurford AJ, Carter A (2003b) Variation in apatite fission-track length measurement: implications for thermal history modeling. Chem Geol 198:77-106

Bertagnolli E, Mark E, Bertel E, Pahl M, Mark TD (1981) Determination of palaeotemperatures of apatite with the fission-track method. Nucl Tracks 5:175-180

Bertel E, Mark TD (1983) Fission tracks in minerals: annealing kinetics, track structure and age correction. Phys Chem Mineral 9:197-204

Bertel E, Mark TD, Pahl M (1977) A new method for the measurement of the mean etchable fission track length and of extremely high fission track densities in minerals. Nucl Track Detection 1:123-126

Bigazzi G (1981) The problem of the decay constant λ_f of ^{238}U. Nucl Tracks 5:35-44

Bonfiglioli G, Ferro A, Mojoni A (1961) Electron microscope investigation on the nature of tracks of fission products in mica. J Appl Phys 32:2499-2503

Brandon MT (1992) Decomposition of fission-track grain-age distributions. Am J Sci 292:535-564
Brix MR, Stockhert B, Seidel E, Theye T, Thomson SN, Kuster M (2002) Thermobarometric data from a fossil zircon partial annealing zone in high pressure-low temperature rocks of eastern and central Crete, Greece. Tectonophys 349:309-326
Burchart J (1981) Evaluation of uncertainties in fission-track dating: some statistical and geochemical problems. Nucl Tracks 5:87-92
Bursill LA, Braunshausen G (1990) Heavy-ion irradiation tracks in zircon. Phil Mag 62:395-420
Burtner RL, Nigrini A, Donelick RA (1994) Thermochronology of Lower Cretaceous source rocks in the Idaho-Wyoming Thrust Belt. Bull Am Assoc Petrol Geol 78:1613-1636
Calk LC, Naeser CW (1973) The thermal effect of a basalt intrusion on fission tracks in quartz monzonite. J Geol 81:189-198
Carlson WD (1990) Mechanisms and kinetics of apatite fission-track annealing. Am Mineral 75:1120-1139
Carlson WD, Donelick RA, Ketcham RA (1999) Variability of apatite fission-track annealing kinetics: I. Experimental results. Am Mineral 84:1213-1223
Carter A (1990) The thermal history and annealing effects in zircons from the Ordovician of North Wales. Nucl Tracks Radiat Meas 17:309-313
Carter A, Moss SJ (1999) Combined detrital-zircon fission-track and U-Pb dating: a new approach to understanding hinterland evolution. Geology 27:235-238
Chadderton LT (2003) Nuclear tracks in solids: registration physics and the compound spike. Radiat Meas 36: 13-34
Chadderton LT, Montagu-Pollock HM (1963) Fission fragment damage to crystal lattices: heat sensitive crystals. Proc Roy Soc A274:239-252
Corrigan JD (1991) Inversion of apatite fission track data for thermal history information. J Geophys Res 96: 10347-10360
Corrigan JD (1993) Apatite fission track analysis of Oligocene strata in South Texas, U.S.A.: Testing annealing models. Chem Geol 104:227-249
Cox R, Kosler J, Sylvester P, Hodych J (2000) Apatite fission-track (FT) dating by LAM-ICO-MS. Abstr. Goldschmidt 2000, Oxford, p 322
Coyle DA, Wagner GA (1998) Positioning the titanite fission-track partial annealing zone. Chem Geol 149: 117-125
Crowley KD (1985) Thermal significance of fission-track length distributions. Nucl Tracks 10:311-322
Crowley KD (1986) Neutron dosimetry in fission-track analysis. Nucl Tracks Radiat Meas 11:237-243
Crowley KD (1993) Lenmodel—a forward model for calculating length distributions and fission-track ages in apatite. Computer Geosci 19:619-626
Crowley KD, Cameron M, Schaefer RL (1991) Experimental studies of annealing of etched fission tracks in fluorapatite. Geochim Cosmochim Acta 55:1449-1465
Donelick RA (1991) Crystallographic orientation dependence of mean etchable fission track length in apatite: An empirical model and experimental observations. Am Mineral 76:83-91
Donelick RA, Miller DS (1991) Enhanced TINT fission track densities in low spontaneous track density apatites using ^{252}Cf-derived fission fragment tracks: a model and experimental observations. Nucl Tracks Radiat Meas 18:301-307
Donelick RA, Farley KA, Asimow P, O'Sullivan PB (2003) Pressure dependence of He diffusion and fission-track annealing kinetics in apatite?: Experimental results. Geochim Cosmochim Acta 67:A82
Donelick RA, Ketcham RA, Carlson WD (1999) Variability of apatite fission-track annealing kinetics: II. Crystallographic orientation effects. Am Mineral 84:1224-1234
Donelick RA, Roden MK, Mooers JD, Carpenter BS, Miller DS (1990) Etchable length reduction of induced fission tracks in apatite at room temperature (~23 °C): Crystallographic orientation effects and initial mean lengths. Nucl Tracks Radiat Meas 17:261-265
Donelick RA, O'Sullivan PB, RA Ketcham (2005) Apatite fission-track analysis. Rev Mineral Geochem 58:49-94
Dumitru TA (2000) Fission-Track Geochronology. In: Quaternary Geochronology: Methods and Applications. Noller JS, Sowers JM, Lettis WR (eds) Am Geophys Union Ref Shelf 4, Washington, DC, American Geophysical Union, p 131-155
Dunlap A, Jaskierowicz G, Jensen J, Della-Negra S (1997) Track separation due to dissociation of MeV C_{60} inside a solid. Nucl Instr Methods B 132:93-98
Durrani IR, Bull RK (1987) Solid State Nuclear Track Detection (Principles, Methods and Application). Pergamon Press, Oxford
Fayon AK (2004) U electron microprobe analyses and monazite fission-track thermochronology. Abstr. 10th International Conference on Fission Track Dating and Thermochronology, Amsterdam, p 36
Fitzgerald P, Gleadow AJW (1990) New approaches in fission track geochronology as a tectonic tool: Examples from the Transantarctic Mountains. Nucl Tracks Radiat Meas 17:351-357
Fleischer RL, Price PB (1963a) Charged particle tracks in glass. J Appl Phys 34:2903-2904